

University of Windsor

Scholarship at UWindor

Electronic Theses and Dissertations

Theses, Dissertations, and Major Papers

2009

Analysis of Self-Excited Synchronous Reluctance Generator

Salah-ud-Din Rana
University of Windsor

Follow this and additional works at: <https://scholar.uwindsor.ca/etd>

Recommended Citation

Rana, Salah-ud-Din, "Analysis of Self-Excited Synchronous Reluctance Generator" (2009). *Electronic Theses and Dissertations*. 8118.
<https://scholar.uwindsor.ca/etd/8118>

This online database contains the full-text of PhD dissertations and Masters' theses of University of Windsor students from 1954 forward. These documents are made available for personal study and research purposes only, in accordance with the Canadian Copyright Act and the Creative Commons license—CC BY-NC-ND (Attribution, Non-Commercial, No Derivative Works). Under this license, works must always be attributed to the copyright holder (original author), cannot be used for any commercial purposes, and may not be altered. Any other use would require the permission of the copyright holder. Students may inquire about withdrawing their dissertation and/or thesis from this database. For additional inquiries, please contact the repository administrator via email (scholarship@uwindsor.ca) or by telephone at 519-253-3000ext. 3208.

Analysis of Self-Excited Synchronous Reluctance Generator

By
Salah-ud-Din Rana

A Thesis
Submitted to the Faculty of Graduate Studies
through the Department of Electrical and Computer Engineering
in Partial Fulfillment of the Requirements for the
Degree of Master of Applied Science at the
University of Windsor

Windsor, Ontario, Canada

2009

© 2009 Salah-ud-Din Rana



Library and Archives
Canada

Published Heritage
Branch

395 Wellington Street
Ottawa ON K1A 0N4
Canada

Bibliothèque et
Archives Canada

Direction du
Patrimoine de l'édition

395, rue Wellington
Ottawa ON K1A 0N4
Canada

Your file *Votre référence*
ISBN: 978-0-494-57578-9
Our file *Notre référence*
ISBN: 978-0-494-57578-9

NOTICE:

The author has granted a non-exclusive license allowing Library and Archives Canada to reproduce, publish, archive, preserve, conserve, communicate to the public by telecommunication or on the Internet, loan, distribute and sell theses worldwide, for commercial or non-commercial purposes, in microform, paper, electronic and/or any other formats.

The author retains copyright ownership and moral rights in this thesis. Neither the thesis nor substantial extracts from it may be printed or otherwise reproduced without the author's permission.

In compliance with the Canadian Privacy Act some supporting forms may have been removed from this thesis.

While these forms may be included in the document page count, their removal does not represent any loss of content from the thesis.

AVIS:

L'auteur a accordé une licence non exclusive permettant à la Bibliothèque et Archives Canada de reproduire, publier, archiver, sauvegarder, conserver, transmettre au public par télécommunication ou par l'Internet, prêter, distribuer et vendre des thèses partout dans le monde, à des fins commerciales ou autres, sur support microforme, papier, électronique et/ou autres formats.

L'auteur conserve la propriété du droit d'auteur et des droits moraux qui protègent cette thèse. Ni la thèse ni des extraits substantiels de celle-ci ne doivent être imprimés ou autrement reproduits sans son autorisation.

Conformément à la loi canadienne sur la protection de la vie privée, quelques formulaires secondaires ont été enlevés de cette thèse.

Bien que ces formulaires aient inclus dans la pagination, il n'y aura aucun contenu manquant.


Canada

**ANALYSIS OF SELF-EXCITED
SYNCHRONOUS RELUCTANCE GENERATOR**

By
Salah-ud-Din Rana

APPROVED BY:

Rupp Carrieavu
Department of Mechanical, Automotive & Materials Engineering

Stephen O'Leary
Department of Electrical and Computer Engineering

Narayan C. Kar, Advisor
Department of Electrical and Computer Engineering

Roberto Muscedere, Chair of Defense
Department of Electrical and Computer Engineering

05 February 2009

AUTHOR'S DECLARATION OF ORIGINALTY

I hereby certify that I am the sole author of this thesis and that parts of this thesis have been published or submitted for publication. I also certify that I have the right to use all or part of the published work in other work.

I certify that, to the best of my knowledge, my thesis does not infringe upon anyone's copyright nor violate any proprietary rights and that any ideas, techniques, quotations, or any other material from the work of other people included in my thesis, published or otherwise, are fully acknowledged in accordance with the standard referencing practices.

I declare that this is a true copy of my thesis, including any final revisions, as approved by my thesis committee and the Graduate Studies office, and that this thesis has not been submitted for a higher degree to any other University or Institution.

ABSTRACT

A steady-state model and a transient model of self-excited synchronous reluctance generator are developed for stand-alone operation. Saturation is considered to predict the actual behavior of the machine. The proposed linearized model is applied to obtain eigenvalues for steady-state stability analysis under different loading conditions. The effects of active, reactive, apparent power output and excitation capacitance on the steady-state performance of self-excited synchronous reluctance generator are analyzed. Eigen value sensitivity is calculated by varying circuit parameters from 50% to 150% of their standard values at 100 μF , 125 μF and 150 μF excitation capacitances. The proposed transient model is applied to observe the transient behavior of machine such as load angle, speed and electromagnetic torque when the machine is subjected to a three-phase symmetrical short-circuit fault across the machine terminals. The load angle sensitivity to machine circuit parameters is investigated.

ACKNOWLEDGEMENTS

I am thankful to Almighty God for giving me the strength and knowledge to complete this research work.

I would like to express my gratitude to my advisor Dr. Narayan C. Kar for his technical guidance, constant encouragement and inspiration throughout the progress of this research work. I believe without his help and advice, it would not have been possible for me to complete this research work. It was a wonderful experience working under his supervision. I would also like to thank my committee members Dr. Rupp Carrieavu and Dr. Stephen O'Leary for their valuable suggestions and guidance in the completion of this research work.

I am thankful to my fellow graduate students for their help, support and encouragement during the progress of this work. During this research work, I had the opportunity to work with other graduate students, attended technical seminars, presentations, conferences which helped me to improve my technical and soft skills. I express my sincere appreciation to all members of Electric Machines and Drives Research Lab for their company and beautiful time which I spent with them.

I thank my wife Sadia, my sons Hassan and Tanzeel and my daughter Zaina for their patience and support throughout this research work.

TABLE OF CONTENTS

AUTHOR'S DECLARATION OF ORIGINALTY	iii
ABSTRACT	iv
DEDICATION	v
ACKNOWLEDGEMENTS	vi
LIST OF TABLES	ix
LIST OF FIGURES	x
LIST OF SYMBOLS	xii
1 INTRODUCTION	1
1.1 Background	1
1.2 Literature Review	2
1.3 Objective	7
1.4 Scope of Work	7
1.5 References	9
2 PROBLEM DEFINITION	13
2.1 Self-Excitation Process	13
2.2 Equivalent Circuit Modeling	14
2.3 Steady-State Modeling	16
2.4 Saturation Modeling	16
2.5 Transient Modeling	17
2.6 Sensitivity Analysis	18
2.7 References	19
3 STEADY-STATE ANALYSIS	21
3.1 Derivation of the Steady-State Model	21
3.2 Stator & Rotor Voltage and Mechanical Equations	24
3.3 Stator and Rotor Flux-Linkages Equations	29
3.4 Saturation Characteristics	30
	vii

3.5	State-Matrix of the System	32
3.6	Calculation of the Elements of the State Matrix	33
3.7	Numerical Analysis	36
3.8	Results of Steady-State Analysis	37
3.9	Sensitivity Analysis to Steady-State Model	42
3.10	Results of Sensitivity Analysis	42
3.11	References	49
4	TRANSIENT ANALYSIS	50
4.1	Transient Model	50
4.2	Transient Stability Analysis Results	53
4.3	Sensitivity Analysis to Transient Model	61
4.4	Results of Sensitivity Analysis	61
5	CONCLUSIONS	66
	LIST OF PUBLICATIONS	68
	VITA AUCTORIS	69

LIST OF TABLES

Table 3.1: Machine parameters	36
Table 3.2: Summary of results: Eigen value sensitivity analysis to steady-state model	48
Table 4.1: Simulation parameters	51
Table 4.2: Load angle swing for longer fault durations	60
Table 4.3: Summary of results: Load angle sensitivity	65

LIST OF FIGURES

Fig. 1.1. Different rotor structures of reluctance machine	4
Fig. 2.1. Voltage build-up process	14
Fig. 2.2. d-axis equivalent circuit	15
Fig. 2.3. q-axis equivalent circuit	15
Fig. 3.1. Phasor diagram of self-excited synchronous reluctance generator	22
Fig. 3.2. Schematic diagram of self-excited synchronous reluctance generator	24
Fig. 3.3. d-axis saturation characteristics	37
Fig. 3.4. Initial value calculation flow chart for steady-state analysis	38
Fig. 3.5. Flow chart for steady-state stability analysis	39
Fig. 3.6. Real parts of eigenvalues corresponding to different active power output for $C=100 \mu\text{F}$ and $Q=0.436 \text{ pu}$	40
Fig. 3.7. Real parts of eigenvalues corresponding to different reactive power output for $C=100 \mu\text{F}$ and $P=0.900 \text{ pu}$	41
Fig. 3.8. Real parts of eigenvalues corresponding to different apparent power demand	41
Fig. 3.9. Real parts of eigenvalues corresponding to different excitation capacitance for $P=0.9 \text{ pu}$ and $Q=0.436 \text{ pu}$	42
Fig. 3.10. Real parts of eigenvalues corresponding to % change in active power	44
Fig. 3.11. Real parts of eigenvalues corresponding to % change in reactive power	44
Fig. 3.12. Real parts of eigenvalues corresponding to % change in d-axis damper circuit resistance	45
Fig. 3.13. Real parts of eigenvalues corresponding to % change in q-axis damper circuit resistance	45
Fig. 3.14. Real parts of eigenvalues corresponding to % change in d-axis damper circuit reactance	46
Fig. 3.15. Real parts of eigenvalues corresponding to % change in q-axis damper circuit reactance	46
Fig. 3.16. Real part of eigenvalues corresponding to % in armature resistance	47
Fig. 3.17. Real parts of eigenvalues corresponding to % change in leakage reactance	47
Fig. 4.1. Transient analysis calculation flowchart	52
Fig. 4.2. Transient variation of load angle	53
Fig. 4.3. Transient variation of rotor speed	54
Fig. 4.4. Transient variation of electromagnetic torque	54
Fig. 4.5. Transient variation of d-axis current	55
Fig. 4.6. Transient variation of q-axis current	56
Fig. 4.7. Transient variation d-axis damper current	56
Fig. 4.8. Transient variation q-axis damper current	57
Fig. 4.9. Transient variation of d-axis flux linkage	57
Fig. 4.10. Transient variation q-axis flux linkage	58
Fig. 4.11. Transient variation of d-axis damper circuit flux linkage	58
Fig. 4.12. Transient variation of q-axis damper circuit flux linkage	59

Fig. 4.13. Load angle swing corresponding to different fault durations	60
Fig. 4.14. Swing in the load angle for different d-axis damper circuit resistance	62
Fig. 4.15. Swing in the load angle for different q-axis damper circuit resistance	62
Fig. 4.16. Swing in the load angle for different d-axis damper circuit reactance	63
Fig. 4.17. Swing in the load angle for different q-axis damper circuit reactance	63
Fig. 4.18. Swing in the load angle for different armature winding resistance	64
Fig. 4.19. Swing in the load angle for different leakage reactance	64

LIST OF SYMBOLS

V_t, V_d, V_q	: Terminal voltage and its d- and q-axis components
X_C	: Capacitive reactance
I_C, I_{cd}, I_{cq}	: Capacitive current and its d- and q-axis components
I_t, I_d, I_q	: Stator current and its d- and q-axis components
I_L, I_{Ld}, I_{Lq}	: Load current and its d- and q-axis components
I_{kd1}, I_{kq1}	: d- and q-axis components of damper circuit current
Ψ_d, Ψ_q	: d- and q-axis components of stator flux linkage
Ψ_{kd1}, Ψ_{kq1}	: d- and q-axis components of damper circuit flux linkage
ω	: Operating speed
ω_0	: Base speed
δ	: Load angle
R_a	: Armature resistance
X_l	: Leakage reactance
R_{kd1}, R_{kq1}	: d- and q-axis damper winding resistances
T_m, T_e	: Mechanical and electromagnetic torques
K_D	: Damping torque coefficient
H	: Inertia constant
X_{mds}, X_{mqs}	: Saturated d- and q-axis reactances
X_{mdu}, X_{mqu}	: Unsaturated d- and q-axis reactances
X_{kd1}, X_{kq1}	: d- and q-axis damper winding reactances
<i>Subscript 0</i>	: Initial operating value of the variables
EV	: Eigen value
r/c	: Real parts of complex eigenvalue

1 INTRODUCTION

1.1 Background

Synchronous generators are the primary source of electric power generation across the globe. The power network mostly depends on synchronous generators. Induction generators are a good alternative to substitute the synchronous generators to produce electrical power over a wide range of speeds. However, their generated voltage and frequency varies with the load and with excitation changes [1]-[3]. Another type of generator which has the same advantages of the induction generators with lower maintenance costs is the synchronous reluctance generator [4].

The primary reason for the popularization of the synchronous reluctance generator is its suitability for wind power generation [5]-[6]. The reluctance generator is a synchronous machine with a specially designed rotor which does not require field excitation. The stator is a conventional polyphase AC stator used for induction and synchronous machines. In rotors, conductors are not required because the torque is produced by the tendency of the rotor to align with the stator produced flux.

A synchronous reluctance generator has the following advantages:

- Rugged and inexpensive
- Robust and simple rotor construction due to the absence of field windings
- Low maintenance requirements
- Core and copper losses are lower
- The frequency of the voltage is independent of load or excitation changes
- Improved voltage regulation by machine design
- Suitable for wind power application

Synchronous reluctance generators can be operated in isolated or grid connected mode. For the grid connected mode, the required excitation is received from the grid. The voltage build-up in the case of a stand-alone synchronous reluctance generator is achieved through self-excitation. Self-excitation in an isolated reluctance generator is achieved when the rotor is driven by the prime mover and its stator terminals are

connected to a suitable capacitor bank. The self-excitation process attains equilibrium due to the action of magnetic saturation [7].

Electrical generators are the backbone of power system, therefore stability analysis of electrical machines are very important. Stability is the ability of an electrical machine for a given initial operating condition, to regain a state of operating equilibrium after being subjected to a physical disturbance. Stability of electrical machines can be affected by steady-state disturbance and transient disturbance. Steady-state stability means the capability of the machine to maintain synchronism under small disturbances. Such disturbances occur because of small variations in loads. Transient stability means the capability of the machine to withstand or survive a sudden change in system characteristics loss of load or faults on the transmission line e.g. symmetrical three-phase short-circuit fault without loss of synchronism [8].

In order to investigate the steady-state and transient stability of reluctance generators, it is important to develop a mathematical model of machine based on the machine equations. A proper machine model can predict the actual machine behavior. The performance of an electrical machine is greatly influenced by the saturation in the magnetic core [9]-[11]. Unsaturated values of the magnetizing reactances in both direct and quadrature axes are reduced as a result of nonlinear behavior of saturation, both for the steady-state and transient modes. To get accurate results from the machine model, the effect of magnetic saturation should be considered [12]-[18]. The effect of saturation is usually ignored in the quadrature axis because of modeling complexity and unavailability of the q-axis saturation characteristics [19]-[21]. For transient analysis, the effect of saturation is generally ignored in both direct and quadrature axes [22].

Sensitivity analysis by varying machine circuit parameters for both the steady-state and transient models of self-excited synchronous reluctance generator can provide valuable information which can assist in the machine design process [23].

1.2 Literature Review

The research on synchronous reluctance machines started in the early 19th century but, in the recent decades, this machine has gained considerable attention due to its

application in wind power generation. The synchronous reluctance generators are strong competitors of induction generators in terms of performance and cost [24]-[25].

Synchronous reluctance machines have attracted considerable attention during the last two decades resulting in much improved performance. In earlier applications, reluctance machines mostly used salient-pole rotor construction while the stator is a conventional stator like the one in an induction machine. To improve the performance of reluctance machines, different rotor construction have been suggested which are as follows:

- Conventional salient-pole
- Segmented rotor
- Axially laminated anisotropic
- Flux-guided or flux-barrier

Most of the literatures on synchronous reluctance machines are related to:

- Self-excitation process to build-up voltage
- Minimum capacitance required for self-excitation process
- Steady-state analysis of grid connected system
- Steady-state analysis for stand-alone system
- Transient analysis
- Eigenvalues sensitivity analysis

Due to the improvements in the electromagnetic design of rotor structures, reluctance machine can be rated equal to induction machine. All the attempts to improve the performance had been centered on modifying rotor magnetic circuits so as to achieve a high X_d/X_q . It is observed that better performance can be achieved by the application of axially laminated rotor structure. The different rotor structures proposed in the literature have been shown in Fig. 1.1 [26]-[29].

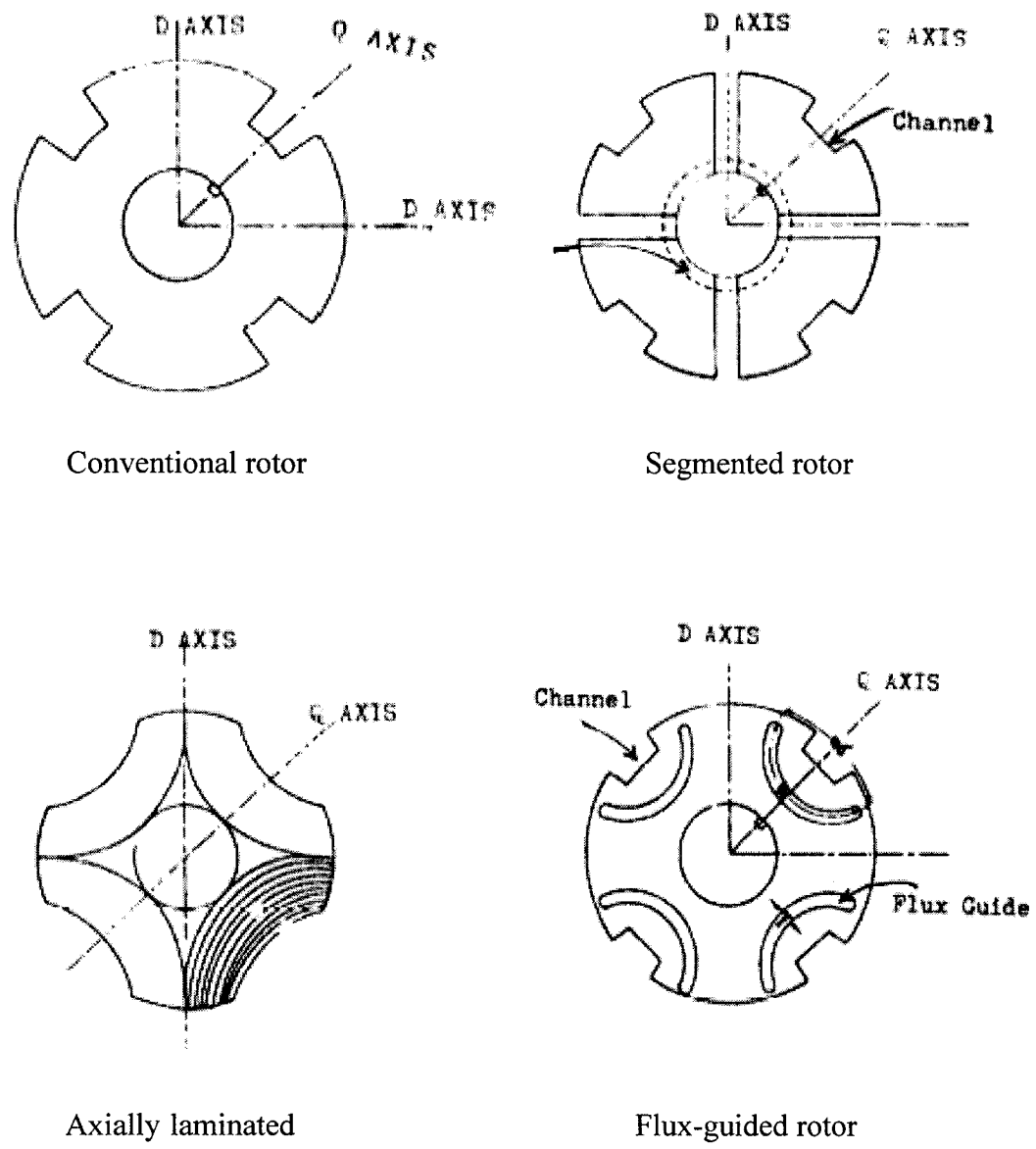


Fig. 1.1. Different rotor structures of reluctance machine.

In [30], I. Boldea, Z.X. Fu, and S.A. Nasar, introduced an axially laminated anisotropic (ALA) rotor for synchronous reluctance machine as a brushless high performance generator. Steady-state performance analysis and the determination of the maximum power-conversion capability of reluctance generators were presented. The high efficiency, high power factor, and high power density of the ALA-rotor reluctance generator are demonstrated through load tests in a laboratory model.

A capacitor bank is a prerequisite for stand-alone operation. In [31], A.I. Aloha, described the capacitance requirements for proper operation of self-excited synchronous reluctance generator and suggested that the excitation capacitance should be slightly greater than the minimum excitation capacitance for better performance. From the analysis, it has been demonstrated that the system efficiency improves with higher capacitance value.

All the steady-state and transient analysis models are based on Park's d- and q-axes equations considering the effect of saturation. Mathematical equations for synchronous reluctance machines can be obtained from the d- and q-axis equivalent circuits. In *abc* axis frame, machine parameters vary with rotor position (θ), making the analysis harder in the *abc* axis frame. Whereas, in the *dq* reference frame, parameters are constant with time or θ . The disadvantage is that only balanced systems can be analyzed using *dq*-axis system.

T.F. Chan [32], presented a general method for analyzing the steady-state performance of a three-phase self-excited reluctance generator with *RL* load. Magnetic saturation is assumed to be confined to the direct axis and is accounted for by a variable direct-axis magnetizing reactance. The system conditions are also measured by using saturation curve.

In [33], a comparison between the steady-state performance of self-excited reluctance and induction generators has been made, the results have shown that reluctance generators have similar operating characteristics as induction generators, in addition to the advantage of operating at a frequency which is independent of load conditions. Earlier attempts have been made to derive a model of reluctance generator by treating it as an induction machine.

In [34], stator core loss has been included in the steady-state modeling of synchronous reluctance motor by C.A.M.D. Ferraz and C.R. de Souza. In [35], A. Boglietti, A. Cavagnino, M. Pastorelli, and A. Vagati, compared the torque behavior between induction and synchronous reluctance motor. The investigation has shown that the reluctance machine can develop 10% to 25% more torque as compared to the induction motor depending upon the motor size and induction motor rotor losses.

V.B. Honsinger performed the steady-state analysis of a poly-phase synchronous reluctance motor. The author developed a method by which the entire motor performance can be calculated [36].

Y.H.A Rahim and M.A.A.S. Alyan [37] performed a transient analysis of a reluctance generator connected to a power system excited by a bank of capacitors. Transient response of excitation capacitor method and load excitation method for load angle sensitivity was discussed.

L. Wang and Y. Wang [38] introduced an eigenvalue and eigenvalue sensitivity method to obtain the minimum loading resistance of an isolated self-excited reluctance generator. The steady-state and dynamic performance of synchronous reluctance generators have been investigated for different loading resistances in order to obtain the minimum loading resistance. Experimental and simulated results of reluctance machine, the effect of sudden switching of various loading resistances on generated voltage have been analyzed. In [39], L. Wang and Y. Wang presented the dynamic performance of sudden connection and disconnection of induction load from self-excited synchronous reluctance generator.

In [4], [31], [32], [37], [38], research works on synchronous reluctance machines are available considering saturation in the direct axis.

In [40], H. Hofman and S.R. Sanders presented a design of a high speed synchronous reluctance machine with minimum eddy current losses in the rotor. Experimental results show an efficiency of 91% at a 10 kW, 10,000 rpm operating point, and negligible rotor heating.

Literature review of previous works provides valuable information on the operating principles and basic machine equations of synchronous reluctance generator. For the better operation and characteristics of synchronous reluctance machines, the

saliency ratio of the rotor has been increased with different rotor structures e.g. salient-pole, segmental and flux guided design.

Capacitance is a prerequisite for the proper operation of self-excited reluctance generator. It has been proven that the efficiency of the system improves with higher capacitance. Steady-state operating limits have been identified to ensure stable performance. Core loss resistance has been included in the modeling of synchronous reluctance machine and a performance analysis has been carried out for *RL* loads. Essential information was obtained on excitation capacitance requirements and steady-state performance of synchronous reluctance generator from the review of these literatures.

Dynamic performance of synchronous reluctance generators has also been studied for a sudden addition or withdrawal of load.

1.3 Objective

The main objective of this research work is to analyze the stability of a synchronous reluctance generator that includes the development of new linearized steady-state and transient models of a self-excited synchronous reluctance generator for stand-alone operation. The stability analysis also depends upon the machine parameters; a sensitivity analysis is required to be performed using the proposed steady-state and transient models of self-excited synchronous reluctance generator.

1.4 Scope of Work

A linearized model of a self-excited synchronous reluctance generator has been developed in order to perform steady-state stability analysis for stand-alone system considering the effect of saturation on the direct axis. The proposed steady-state model is based upon the following assumptions:

- Core losses has been neglected
- Voltage and current harmonics have been neglected

This research is focused on the development of a new linearized and accurate model for the self-excited synchronous reluctance generator for stand-alone operation. The model is based upon the Park's d-q axes equations. Using the generator stator and

rotor voltage, flux linkage, torque and mechanical equations, a linearized model has been developed by applying the small perturbation technique. The saturation has been represented by modifying the unsaturated magnetizing reactance with a saturation factor S_d . The developed model has been applied to obtain eigenvalues under different operating conditions. By using this model, the effects of excitation capacitance, real, reactive and apparent power output on the steady-state stability of the self-excited synchronous reluctance generator have been investigated. A sensitivity analysis has been performed by varying the machine parameters from 50% to 150% with a step 10% increase of their original values.

The transient model has been developed by using generator stator, rotor and mechanical equations. A three-phase symmetrical short-circuit fault was initiated to predict the transient behavior of self-excited synchronous reluctance generator. Transient variations of load angle, speed, electromagnetic torque and other parameters have been investigated to analyze the transient performance of the self-excited synchronous reluctance generator. Load angle sensitivity to transient model has been carried out by varying the machine parameters from 50% to 150% of their standard values at 100 μ F excitation capacitance.

1.5 References

- [1] A.K. Tandon, S.S. Murthy, and G.J. Berg, "Steady-state analysis of capacitor self-excited induction generators," *IEEE Trans. Power Apparatus and Systems*, PAS-103, pp. 612-618, Mar. 1984.
- [2] A. K. Mohanty and M. K. Khanijo, "Circuit theory of reluctance machines," *IEEE Trans. Power Apparatus and Systems*, PAS-88, pp.937-944, June 1969.
- [3] N.H. Malik and A.H. Al-Bahrani, "Influence of the terminal capacitor on the performance characteristics of a self-excited induction generator," *IEEE Proc.* vol.137, pp.168-193, Mar. 1990.
- [4] A.L. Mohamadein, Y.H.A. Rahim, and A.S. Al-Khalaf, "Steady-state performance of a self-excited reluctance generator," *IEE Proc. Electric Power Application*, vol.138, pp. 193-198, May 1991.
- [5] S. Guha and N.C. Kar, "A linearized model of saturated self-excited synchronous reluctance generator," in *Proc. 2005 IEEE CCECE*, pp. 633-636.
- [6] S. Ghua, H. Soloumah, and N.C. Kar, "Status of and prospect for wind power generation in Canada," *Wind Engineering*, vol.29, pp. 253-270, 2005.
- [7] A.I. Aloha, "Steady-state operating limits of three-phase self-excited induction and reluctance generator," *IEE Proc. Generation, Transmission and Distribution*, vol. 139, pp. 261-268, May 1992.
- [8] P. Kundur, "*Power System Stability and Control*," McGraw-Hill Inc.: New York, 1994.
- [9] A.M. El-Serafi and A.S. Abdallah, "Effect of saturation on the steady-state stability of a synchronous machine connected to an infinite bus system," *IEEE Trans. Energy Conversion*, vol.6, pp.514-521, Sep. 1991.
- [10] A.M. El-Serafi and A.S. Abdallah, "Saturated synchronous reactances of synchronous machines," *IEEE Trans. Energy Conversion*, vol.7, pp.570-579, Sep. 1992.
- [11] A.M. El-Serafi, A.S. Abdallah, M.K. El-Sherbiny, and E.H Badawy, "Experimental study of the saturation and cross-magnetizing phenomenon in saturated synchronous machines," *IEEE Trans. Energy Conversion*, vol.3, pp.815-823, Dec. 1988.

- [12] S. Bhadra, "A direct method to predict instantaneous saturation curve from rms saturation curve," *IEEE Trans. Magnetics*, vol.18, pp.1867-1870, Nov. 1982.
- [13] S. Ramshaw and G. Xie, "Nonlinear model of non-salient synchronous machines," *IEEE Trans. Power Apparatus and Systems*, PAS-103, pp.1809-1815, July 1984.
- [14] J.E. Brown, K.P. Kovacs, and P. Vas, "A method of including the effects of main flux path saturation in the generalized equations of ac machines," *IEEE Trans. Power Apparatus and Systems*, PAS-102, pp.96-103, Jan. 1983.
- [15] E. Levi, "Modelling of magnetic saturation in smooth air-gap synchronous machine," *IEEE Trans. Energy Conversion*, vol.12, pp.151-156, June 1997.
- [16] E. Levi, "A unified approach to main flux saturation modeling in d-q axis models of induction machines," *IEEE Trans. Energy Conversion*, vol.10, pp.455-461, Sep. 1995.
- [17] J.O. Ojo and T.A. Lipo, "An improved model for saturated salient-pole synchronous motors," *IEEE Trans. Energy Conversions*, vol.4, pp.135-142, Mar. 1989.
- [18] S.D. Pekarek, E.A. Walters and B.T. Kuhn, "An efficient method of representing saturation in physical variable models of synchronous machines," *IEEE Trans. Energy Conversion*, vol.14, pp. 72-79, Mar. 1999.
- [19] F. Wang, "A nonlinear saturation model for salient-pole synchronous machines in high performance drive applications," *Proc. of the Industry Applications Conference*, 38th IAS Annual Meeting, vol.2, pp. 906-910, Oct. 2003.
- [20] S.M. Allam, M.A. El-Khazendar, and A.M. Osheiba, "Steady-state analysis of a self-excited single-phase reluctance generator," *IEEE Trans. Energy Conversion*, vol.22, pp. 584-591, Sep. 2007.
- [21] Y. Wang and L. Wang, "Steady-state performance of a self-excited reluctance generator under unbalanced excitation capacitors," *IEEE Power Engineering Society*, vol.1, pp. 281-285, Jan. 2000.
- [22] Y.H.A. Rahim and A.M.L. Al-Sabbagh, "Controlled power transfer from wind driven reluctance generator," *IEEE Trans. Energy Conversion*, vol.7, pp. 275-281, Dec. 1997.

- [23] N.C. Kar and J. Tamura, "Effects of synchronous machine saturation, circuit parameters, and control systems on steady-state stability," *Electric Machines and Power Systems*, pp. 327-342, 1999.
- [24] A. Kilthau and J.M. Pacas, "Appropriate models for the control of the synchronous reluctance machine," *Record of the 2002, Industry conference Applications*, pp.2289-2295.
- [25] N. Ben-Hali and R. Rabinovici, "Three-phase autonomous reluctance generator," *IEE Proc. Electric Power Applications*, vol.148, pp. 438-442, Sep. 2001.
- [26] M.H. Nagrial and M.A. Rahman, "Operation and characteristics of self-excited reluctance generator," *IEEE Industry Applications Society Annual Meeting*, vol.1, pp. 55-58, Oct. 1988.
- [27] P.J. Lawrenson and L.A. Agu, "Theory and performance of polyphase reluctance machines," *IEEE Proc.*, vol.111, pp. 1435-1445, Aug. 1964.
- [28] T. Matsuo and T.A. Lipo, "Rotor design optimization of synchronous reluctance machine," *IEEE Trans. Energy Conversion*, vol.9, pp. 359-365, June, 1994.
- [29] E. Schmidt, W. Brandl, and C. Grabner, "Design improvement of synchronous reluctance machines with internal rotor flux barriers for high speed drives," *Proc. of the IEEE 33rd Annual Power Electronics Specialists Conference*, vol.4, pp. 1949-1954, June 2002.
- [30] I. Boldea, Z.X. Fu, and S.A. Nasar, "High-performance reluctance generator," *IEE Proc. Electric Power Applications*, vol.140, pp. 124-130, Mar. 1993.
- [31] A.I. Alolah, "Capacitance requirements for three-phase self-excited reluctance generator," *IEE Proc. Generation, Transmission and Distribution*, vol.138, pp. 193-198, May 1991.
- [32] T.F. Chan, "Steady-state analysis of a three-phase self-excited reluctance generator," *IEEE Trans. Energy Conversion*, vol.7, pp. 223-230, Mar. 1992.
- [33] Y.H.A. Rahim, A.L. Mohamadein, and A.S. Al-khalaf, "Comparison between the steady-state performance of self-excited reluctance and induction generators," *IEEE Trans. Energy Conversion*, vol.5, pp.519-525, Sep. 1990.

- [34] C.A.M.D. Ferraz and C.R. de Souza, "Considering from core losses in modeling the reluctance synchronous motors," *7th International Workshop on Advanced Motion Control*, pp. 251-256, July 2002.
- [35] A. Boglietti, A. Cavagnino, M. Pastorelli, and A. Vagati, "Experimental comparison of induction and synchronous reluctance motors performance," *Proc. of the Industrial Application Conference, 40th IAS Annual Meeting*, vol. 1, pp. 474-479, October 2005.
- [36] V.B. Honsinger, "Steady-state performance of reluctance machines," *IEEE Trans. Power Apparatus and Systems*, PAS-90, pp. 305-311, Jan. /Feb. 1971.
- [37] Y.H.A. Rahim and M.A.A.S. Alyan, "Effect of excitation capacitors on transient performance of reluctance generators," *IEEE Trans. Energy Conversion*, vol.6, pp.714-720, Dec. 1991.
- [38] Y.-S. Wang and L. Wang, "Minimum loading resistance and its effects on performance of an isolated self-excited reluctance generator," *IEE Proc. Generation, Transmission and Distribution*, vol.148, pp. 251-256, May 2001.
- [39] Y.-S. Wang and L. Wang, "Characteristics of a self-excited reluctance generator as effected by sudden connection of an induction motor load," *Proc. of the International Conference Power System Technology*, vol.1, pp. 605-6096, Aug. 1998.
- [40] H. Hofmann and S. R. Sanders, "High-speed synchronous reluctance machine with minimized rotor losses," *IEEE 33th IAS Meeting Industry Application Conference*, pp.118-126, 1998.

2 PROBLEM DEFINITION

2.1 Self-Excitation Process

A synchronous reluctance generator can be operated in either isolated or grid connected mode. In the case of the grid connected mode, the required excitation is received from the grid. In the stand-alone operation, the excitation can be provided by the capacitance connected across the stator terminals of the generator.

This research is focused on a synchronous reluctance generator for a stand-alone operation. The terminal voltage builds up by the action of self-excitation. When the rotor is rotated using an external prime mover, the small residual flux in the rotor creates voltage across the stator terminals. The same voltage is also applied to a bank of capacitor causing a flow of small capacitive current. The small capacitive current flows through the stator windings creating more flux which adds the residual flux in order to increase the voltage level. An increase in voltage level increases the current which in turns increases the voltage at the terminals. This process continues until a stable point is reached depending upon the degree of magnetic saturation and external capacitance. The reactive power required for the load is supplied by a bank of capacitor whereas the active power is supplied by the generator [1]-[3].

The machine reaches the steady-state condition with the particular load current and terminal voltage, if saturation is considered. This is determined by the real and reactive power flow between the machine, the excitation capacitance and the connected load. For the unsaturated case, the voltage build-up does not terminate and the terminal voltage continues to grow as the equilibrium condition is never satisfied. A typical self-excitation phenomenon is shown in Fig. 2.1.

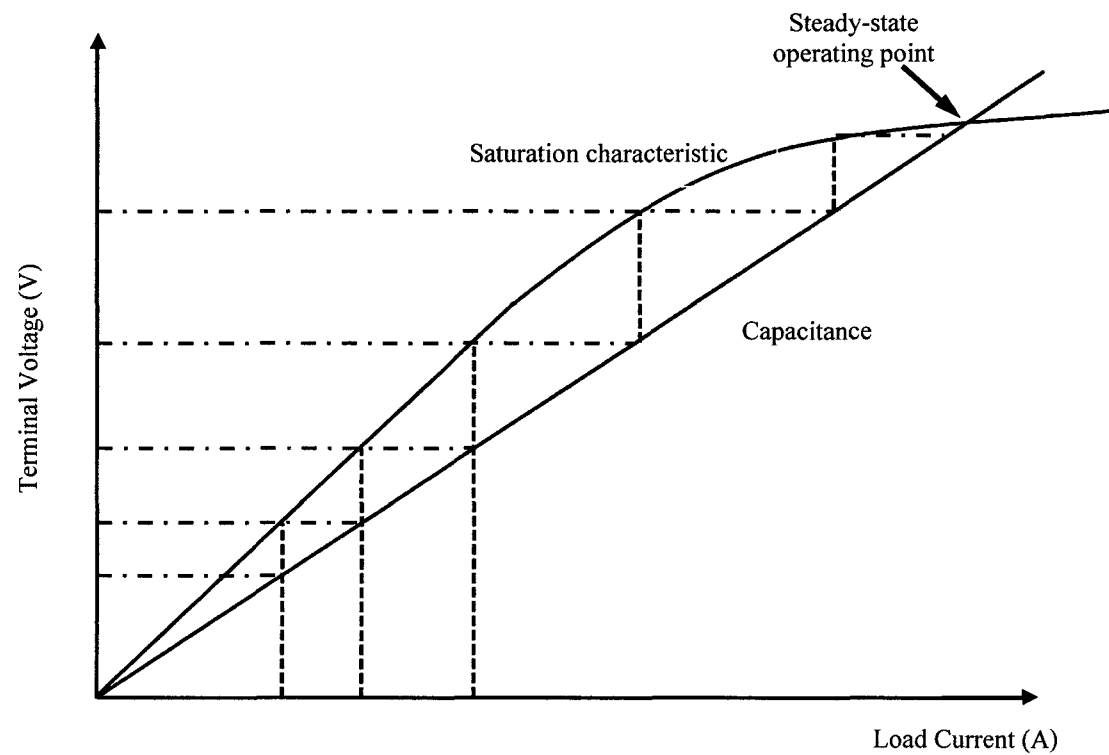


Fig. 2.1. Voltage build-up process.

2.2 Equivalent Circuit Modeling

The d- and q-axis equivalent circuits of a self-excited synchronous reluctance generator are shown in Fig. 2.2 and Fig. 2.3. One damper winding in the direct axis and one damper winding in the quadrature axis have been considered with the external capacitance connected across the stator terminals of the generator.

The following assumptions are made for the development of machine model:

- Core losses are neglected
- The induced voltage and current harmonics are neglected
- Saturation is considered in the direct axis

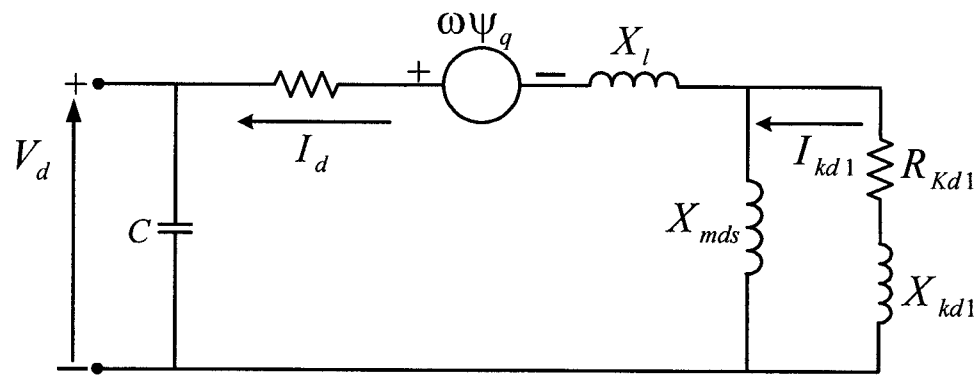


Fig. 2.2. d-axis equivalent circuit.

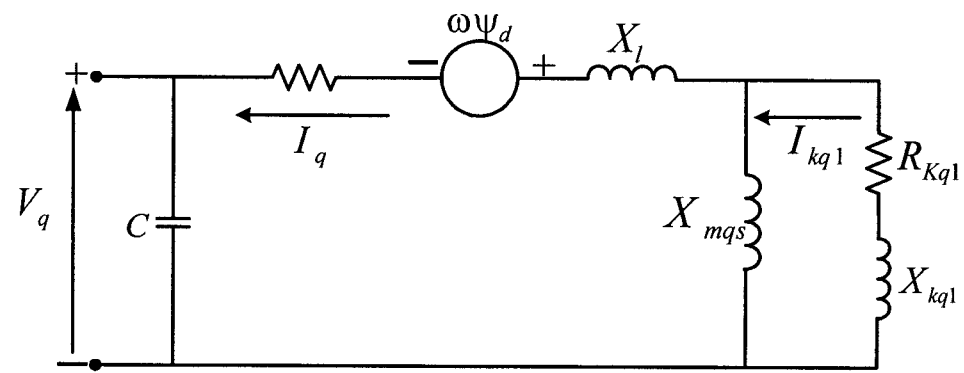


Fig. 2.3. q-axis equivalent circuit.

2.3 Steady-State Modeling

Steady-state stability is the ability of the machine to remain in synchronism when subjected to small disturbances. A small disturbance is a disturbance for which the set of equations describing the generator may be linearized for the purpose of analysis. The instability can be classified as follows [4]:

- Steady increase in generator rotor angle
- Rotor oscillations
- Gradual changes in loads
- Irregularities in prime-mover input, etc.

Study of steady-state stability provides information about the dynamic characteristics of different machine components. The purpose of steady-state stability is one of the following.

- Post-disturbance analysis
- Power system planning
- Power system operation

In this research work, a linearized steady-state model of self-excited synchronous reluctance generator is developed by using the Park's d-q axes equations, considering one damper in the direct axis and one in the quadrature axis. Using the stator and rotor voltage, flux linkage, torque and mechanical equations, a linearized steady-state model has been developed by applying the small perturbation technique. The saturation has been represented by modifying the unsaturated magnetizing reactance with a saturation factor. The developed model has been applied to obtain eigenvalues under different operating conditions. By using the steady-state model, the effects of excitation capacitance, real, reactive and apparent power output on the steady-state stability of the self-excited synchronous reluctance generator has been analyzed.

2.4 Saturation Modeling

The effect of saturation on electrical machine steady-state performance has been recognized for at least 60 years when the initial concern was the accuracy of the calculation of machine performance. For the steady-state and transient modeling of self-

excited synchronous reluctance generators, the effect of saturation should be considered to predict the actual behavior of the machine. The accurate calculation of the performance of AC machines is mostly dependent on the saturation conditions.

Most machines models employ piece-wise linearization technique [5], [6] and polynomial function [7], [8] to represent the saturation curves. Different authors have proposed different methods to model saturation for electrical machines. Some machine models have considered the effects of saturation in both direct and quadrature axes and the magnetic coupling between d- and q-axis windings (cross-magnetizing phenomenon) [9].

The values of d- and q-axis saturated magnetizing reactances, $X_{m ds}$ and $X_{m qs}$ are obtained by modifying their unsaturated values as follows:

$$X_{m ds} = S_d \cdot X_{m du} \quad (2.1)$$

$$X_{m qs} = S_q \cdot X_{m qu} \quad (2.2)$$

Where S_d and S_q are the d- and q-axis saturation factors, respectively.

The saturated values can be obtained by using the polynomial equation from the saturation characteristics of the machine model.

A significant reduction in the values of magnetizing reactances in both direct and quadrature axes from their corresponding unsaturated values have been observed as a result of nonlinearities introduced by saturation under both steady-state and transient operations [10]. Thus, in the modeling of synchronous reluctance generator, a proper representation of saturation is importance for an accurate steady-state and transient stability analysis of the machine.

2.5 Transient Modeling

Transient stability means the ability of the machine to survive a sudden change in system characteristics such as:

- Loss of a load
- Loss of excitation
- Faults on the transmission line

In the transient stability studies, the important issues are as follows [11]:

- Calculation of generator load angle or torque during the fault period.
- Calculation of post-fault generator load angle, for a period of up to several seconds after the fault cleared.

The transient performance of synchronous reluctance generators under fault can be observed by solving machine differential equations, to obtain the values of the fluxes, currents, load angle, speed and torque in each time step. In each time step, a 4th order Runge-Kutta method has been employed to solve differential equations using the coefficients of Runge-Kutta method and the value of parameters from the previous time step. The newly obtained values are then used as the initial values for the next time step. At the clearance of the fault, the terminal voltage is again restored to its original value. For a stable system, after a few oscillations, the system reaches equilibrium and the parameters are restored to their original values. This involves an iterative process and after the currents converge it proceeds to the next time step [12], [13]. The calculated currents, flux linkages, speed and load angle at the end of the each time step can be used to find the transient performance for the next time step.

2.6 Sensitivity Analysis

A sensitivity analysis has been performed using the developed steady-state model by varying the parameters from 50% to 150% with a step 10% increase with different excitation capacitances 100 μ F, 125 μ F and 150 μ F of their standard value.

A sensitivity analysis has been carried out to transient model by varying the machine parameters for 50%, 75%, 100%, 125% and 150% of their standard value with 100 μ F excitation capacitance. Load angle sensitivity to machine parameters has been analyzed using the developed transient model of self-excited reluctance generator.

2.7 References

- [1] T.F. Chan, "Steady-state analysis of a three-phase self-excited reluctance generator," *IEEE Trans. Energy Conversion*, vol.7, pp. 223-230, Mar. 1992.
- [2] T.F. Chan, "Analysis of self-excited induction generators using an iterative method," *IEEE Trans. Energy Conversion*, vol.10, pp. 502-507, Sep. 1995.
- [3] M.H. Nagrial and M.A. Rahman, "Operation and characteristics of self-excited reluctance generator," *IEEE Industry Applications Society Annual Meeting*, vol.1, pp. 55-58, Oct. 1988.
- [4] P. Kundur, "*Power System Stability and Control*," McGraw-Hill Inc., New York, 1994.
- [5] Y.-S. Wang and L. Wang, "Minimum loading resistance and its effects on performance of an isolated self-excited reluctance generator," *IEE Proc. Generation, Transmission and Distribution*, vol. 148, pp. 251-256, May 2001.
- [6] Y.-S. Wang and L. Wang, "Characteristics of a self-excited reluctance generator as effected by sudden connection of an induction motor load," *Proc. of the International Conference Power System Technology*, vol.1, pp. 605-609, Aug. 1998.
- [7] O. Ojo, "Limit cycle and small signal dynamics of self-excited synchronous reluctance generator," *Proc. of the 26th Southeastern Symposium on System Theory*, pp. 244-248, Mar. 1994.
- [8] N. Ben-Hali and R. Rabinovici, "Three-phase autonomous reluctance generator," *IEE Proc. Electric Power Applications*, vol.148, pp. 438-442, Sep. 2001.
- [9] A.M. El-Serafi, A.S. Abdallah, M.K. El-Sherbiny and E.H Badawy, "Experimental study of the saturation and cross-magnetizing phenomenon in saturated synchronous machines," *IEEE Trans. Energy Conversion*, vol.3, pp.815-823, Dec. 1988.
- [10] A.M. El-Serafi and A.S. Abdallah, "Saturated synchronous reactances of synchronous machines," *IEEE Trans. Energy Conversion*, vol.7, pp.570-579, Sep. 1992.
- [11] *IEEE Guide for Synchronous Generator Modeling Practices and Applications in Power System Stability Analyses*, IEEE STD. 1110-1991, 2002

- [12] Y.H.A. Rahim and M.A.A.S. Alyan, "Effect of excitation capacitors on transient performance of reluctance generators," *IEEE Trans. Energy Conversion*, vol.6, pp.714-720, Dec. 1991.
- [13] S. Ghua and N.C. Kar, "Saturation modeling and stability analysis of synchronous reluctance generator," *IEEE Trans. Energy Conversion*, vol.23, Sep. 2008.

3 STEADY-STATE ANALYSIS

3.1 Derivation of the Steady-State Model

The phasor diagram of the self-excited synchronous reluctance generator with a capacitor bank connected across the stator terminals of a machine for a lagging load is shown in Fig. 3.1. The phasor diagram describes the steady-state operating condition of the machine. The stator current is the phasor sum of the load current and capacitor current. The stator current is resolved into its d- and q-axis components. Similarly, the voltages and currents have been resolved into their corresponding d- and q-axis components. All the resistive and reactive voltage drops are shown in the Phasor diagram.

A linearized model of self-excited synchronous reluctance generator has been developed for stand-alone operation using the machine voltage, mechanical and flux linkage differential equations. It is based upon Park's d-q axes equations considering one damper winding in the direct axis and one damper winding in the quadrature axis. The effect of saturation is considered in the direct-axis [1]-[3]. From the phasor diagram shown in Fig. 3.1, the terminal voltage in (3.1) can be resolved into its d- and q-axis components as follows:

$$V_t = V_d + jV_q \quad (3.1)$$

where

$$V_d = V_t \sin \delta \quad (3.2)$$

and

$$V_q = V_t \cos \delta \quad (3.3)$$

Linearizing (3.2)-(3.3) by using Taylor series approximation, (3.4)-(3.5) can be obtained.

$$\Delta V_d = V_{t0} \cos \delta_0 \Delta \delta + \Delta V_t \sin \delta_0 \quad (3.4)$$

$$\Delta V_q = V_{t0} \sin \delta_0 \Delta \delta + \Delta V_t \cos \delta_0 \quad (3.5)$$

As the capacitors are connected across the stator terminals of the machine, the same terminal voltage will be applied across the capacitors. The current flowing through the capacitors will lead the terminal voltage by 90° and its magnitude can be written:

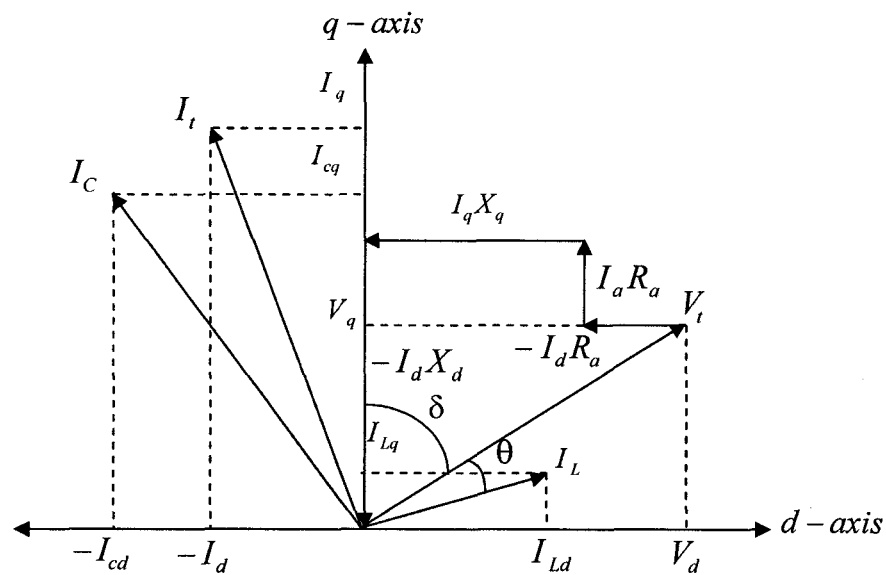


Fig. 3.1. Phasor diagram of self-excited synchronous reluctance generator.

$$I_C = \frac{V_t}{jX_c} \quad (3.6)$$

(3.6) can be re-written as

$$I_C = \frac{V_d + jV_q}{jX_c} \quad (3.7)$$

Resolving the capacitive current into its corresponding d- and q-axis components, the following equation can be obtained.

$$I_C = I_{cd} + jI_{cq} \quad (3.8)$$

Using (3.2) and (3.3) in (3.7), the capacitive current can be written as follows:

$$I_C = \frac{V_t}{X_c} \cos\delta - j \frac{V_t}{X_c} \sin\delta \quad (3.9)$$

Equating (3.8) and (3.9), d- and q-axis components of the capacitive current can be expressed in terms of d- and q-axis voltages as follows:

$$I_{cd} = \frac{V_t}{X_c} \cos\delta \quad (3.10)$$

$$I_{cq} = -\frac{V_t}{X_C} \sin \delta \quad (3.11)$$

Linearizing (3.10)-(3.11) using Taylor's series approximation, (3.12) and (3.13) can be obtained.

$$\Delta I_{cd} = -\frac{V_{t0}}{X_C} \sin \delta_0 \Delta \delta + \frac{1}{X_C} \cos \delta_0 \Delta V_t \quad (3.12)$$

$$\Delta I_{cq} = -\frac{V_{t0}}{X_C} \cos \delta_0 \Delta \delta - \frac{1}{X_C} \sin \delta_0 \Delta V_t \quad (3.13)$$

Arranging (3.12)-(3.13) in matrix form, (3.14) can be obtained.

$$\begin{bmatrix} \Delta I_{cd} \\ \Delta I_{cq} \end{bmatrix} = \begin{bmatrix} -\frac{V_{t0}}{X_C} \sin \delta_0 \\ -\frac{V_{t0}}{X_C} \cos \delta_0 \end{bmatrix} [\Delta \delta] + \begin{bmatrix} \frac{1}{X_C} \cos \delta_0 \\ -\frac{1}{X_C} \sin \delta_0 \end{bmatrix} [\Delta V_t] \quad (3.14)$$

From the schematic diagram as shown in Fig. 3.2, the capacitive current can be expressed in terms of stator current and load current as follows:

$$I_C = I_t - I_L \quad (3.15)$$

Resolving the capacitive current into its corresponding d- and q-axis components, the following equations can be obtained.

$$I_{cd} = I_d - I_{Ld} \quad (3.16)$$

$$I_{cq} = I_q - I_{Lq} \quad (3.17)$$

Linearizing (3.16) and (3.17), (3.18) and (3.19) can be obtained.

$$\Delta I_{cd} = \Delta I_d - \Delta I_{Ld} \quad (3.18)$$

$$\Delta I_{cq} = \Delta I_q - \Delta I_{Lq} \quad (3.19)$$

Replacing (3.14) with the values of linearized d- and q-axis capacitive currents into (3.18) and (3.19), (3.20) and (3.21) can be obtained.

$$\Delta I_d = \Delta I_{Ld} - \frac{V_{t0}}{X_C} \sin \delta_0 \Delta \delta + \frac{1}{X_C} \cos \delta_0 \Delta V_t \quad (3.20)$$

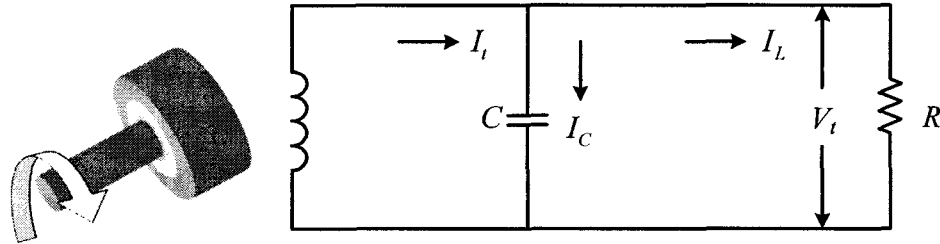


Fig. 3.2. Schematic diagram of self-excited synchronous reluctance generator.

$$\Delta I_q = \Delta I_{Lq} - \frac{V_{t0}}{X_C} \cos \delta_0 \Delta \delta - \frac{1}{X_C} \sin \delta_0 \Delta V_t \quad (3.21)$$

The damper winding currents in the generator are independent of load angle changes. Using (3.20)-(3.21) and linearized d- and q-axis damper winding currents, the generator currents can be written in matrix form as given below:

$$\begin{bmatrix} \Delta I_d \\ \Delta I_{kd1} \\ \Delta I_q \\ \Delta I_{kq1} \end{bmatrix} = \begin{bmatrix} \Delta I_{Ld} \\ \Delta I_{kd1} \\ \Delta I_{Lq} \\ \Delta I_{kq1} \end{bmatrix} - \left(\begin{bmatrix} \frac{V_{t0}}{X_C} \sin \delta_0 \\ 0 \\ \frac{V_{t0}}{X_C} \cos \delta_0 \\ 0 \end{bmatrix} [\Delta \delta] - \begin{bmatrix} \frac{1}{X_C} \cos \delta_0 \\ 0 \\ \frac{-1}{X_C} \sin \delta_0 \\ 0 \end{bmatrix} [\Delta V_t] \right) \quad (3.22)$$

(3.22) can be re-written as follows:

$$[\Delta I_T] = [\Delta I] - [\Delta I_C] \quad (3.23)$$

3.2 Stator & Rotor Voltage and Mechanical Equations

The self-excited synchronous reluctance generator model has been developed by considering one damper winding on the direct axis and one on the quadrature axis. The stator and rotor voltage equations can be written as follows:

$$d\psi_d/dt = \omega_0 V_d + \omega_0 R_a I_d + \omega \psi_q \quad (3.24)$$

$$d\psi_q/dt = \omega_0 V_q + \omega_0 R_a I_q - \omega \psi_d \quad (3.25)$$

$$\frac{d\psi_{kd1}}{dt} = -\omega_0 R_{kd1} I_{kd1} \quad (3.26)$$

$$\frac{d\psi_{kq1}}{dt} = -\omega_0 R_{kq1} I_{kq1} \quad (3.27)$$

The mechanical equation can be expressed as follows:

$$\frac{d\delta}{dt} = \omega - \omega_0 \quad (3.28)$$

$$\frac{d\omega}{dt} = \frac{\omega_0}{2H} [T_m - T_e - K_D \omega] \quad (3.29)$$

The electromagnetic torque equation can be expressed in terms of the stator flux-linkages and currents.

$$T_e = (\psi_d I_q - \psi_q I_d) \quad (3.30)$$

Linearizing (3.24), d-axis stator flux linkage as follows:

$$\frac{d(\Delta\psi_d)}{dt} = \omega_0 \Delta V_d + \omega_0 R_a \Delta I_d + \omega_0 \Delta\psi_q + \psi_{q0} \Delta\omega$$

$$\frac{d(\Delta\psi_d)}{dt} = \omega_0 \Delta V_d + \omega_0 R_a (\Delta I_{Ld} + \Delta I_{cd}) + \omega_0 \Delta\psi_q + \psi_{q0} \Delta\omega$$

Replacing the values of the linearized d-axis capacitive current and d-axis voltage in the above equation.

$$\begin{aligned} \frac{d(\Delta\psi_d)}{dt} &= \omega_0 (V_{i0} \cos \delta_0 \Delta\delta + \sin \delta_0 \Delta V_i) + \omega_0 R_a \Delta I_{Ld} \\ &\quad + \omega_0 R_a \left(-\frac{V_{i0}}{X_C} \sin \delta_0 \Delta\delta + \frac{1}{X_C} \cos \delta_0 \Delta V_i \right) + \omega_0 \Delta\psi_q + \psi_{q0} \Delta\omega \\ \frac{d(\Delta\psi_d)}{dt} &= \omega_0 \Delta\psi_q + \omega_0 V_{i0} \left(\cos \delta_0 - \frac{R_a}{X_C} \sin \delta_0 \right) \Delta\delta + \omega_0 R_a \Delta I_{Ld} \\ &\quad + \omega_0 \left(\sin \delta_0 + \frac{R_a}{X_C} \cos \delta_0 \right) \Delta V_i + \psi_{q0} \Delta\omega \\ \frac{d(\Delta\psi_d)}{dt} &= \omega_0 \Delta\psi_q + \omega_0 V_{i0} \left(\cos \delta_0 - \frac{R_a}{X_C} \sin \delta_0 \right) \Delta\delta + \omega_0 R_a \Delta I_{Ld} + \\ &\quad \omega_0 \left(\sin \delta_0 + \frac{R_a}{X_C} \cos \delta_0 \right) \Delta V_i + \psi_{q0} \Delta\omega \end{aligned} \quad (3.31)$$

Similarly, Linearizing (3.25), q-axis stator flux linkage equation.

$$\frac{d(\Delta\psi_q)}{dt} = \omega_0 \Delta V_q + \omega_0 R_a \Delta I_q - \omega_0 \Delta\psi_d - \psi_{d0} \Delta\omega$$

$$\frac{d(\Delta\psi_q)}{dt} = \omega_0 (-V_{t0} \sin \delta_0 \Delta\delta + \cos \delta_0 \Delta V_t) + \omega_0 R_a (\Delta I_{Lq} + \Delta I_{cq}) - \omega_0 \Delta\psi_d - \psi_{d0} \Delta\omega$$

Substituting the values of the linearized q-axis capacitive current and voltage in the above equation.

$$\begin{aligned} \frac{d(\Delta\psi_q)}{dt} = & -\omega_0 \Delta\psi_d - \omega_0 V_{t0} \left(\sin \delta_0 + \frac{R_a}{X_C} \cos \delta_0 \right) \Delta\delta + \omega_0 R_a \Delta I_{Lq} + \\ & \omega_0 \left(\cos \delta_0 - \frac{R_a}{X_C} \sin \delta_0 \right) \Delta V_t - \psi_{d0} \Delta\omega \end{aligned} \quad (3.32)$$

Linearizing d- and q-axis damper flux linkages, (3.26) and (3.27) respectively, (3.33) and (3.34) can be obtained in the linearized form.

$$\frac{d(\Delta\psi_{kd1})}{dt} = -\omega_0 R_{kd1} \Delta I_{kd1} \quad (3.33)$$

$$\frac{d(\Delta\psi_{kq1})}{dt} = -\omega_0 R_{kq1} \Delta I_{kq1} \quad (3.34)$$

Linearizing (3.28) and (3.29), load angle and speed equations, (3.35) and (3.36) can be obtained as follow:

$$\frac{d(\Delta\delta)}{dt} = \Delta\omega \quad (3.35)$$

$$\frac{d(\omega)}{dt} = \frac{\omega_0}{2H} [\Delta T_m - \Delta T_e - K_D \Delta\omega] \quad (3.36)$$

Linearizing (3.30), the electromagnetic torque equation.

$$T_e = \psi_{d0} (\Delta I_{Lq} + \Delta I_{cq}) + I_{q0} \Delta\psi_d - \psi_{q0} (\Delta I_{Ld} + \Delta I_{cd}) - I_{d0} \Delta\psi_q$$

$$T_e = \psi_{d0} \Delta I_{Lq} + \psi_{d0} (\Delta I_{cq}) + I_{q0} \Delta\psi_d - \psi_{q0} \Delta I_{Ld} - \psi_{q0} (\Delta I_{cd}) - I_{d0} \Delta\psi_q$$

Substituting the values of linearized currents in the above equation.

$$T_e = \psi_{d0} \Delta I_{Lq} + \psi_{d0} \left(-\frac{V_{t0}}{X_C} \cos \delta_0 \Delta \delta - \frac{1}{X_C} \sin \delta_0 \Delta V_t \right) + I_{q0} \Delta \psi_d - \psi_{q0} \Delta I_{Ld} - \psi_{q0} \left(-\frac{V_{t0}}{X_C} \sin \delta_0 \Delta \delta + \frac{1}{X_C} \cos \delta_0 \Delta V_t \right) - I_{d0} \Delta \psi_q$$

(3.37) can be written as follows:

$$T_e = \psi_{d0} \Delta I_{Lq} - \frac{V_{t0}}{X_C} (\psi_{d0} \cos \delta_0 + \psi_{q0} \sin \delta_0) \Delta \delta - \frac{1}{X_C} (\psi_{d0} \sin \delta_0 + \psi_{q0} \cos \delta_0) \Delta V_t + I_{q0} \Delta \psi_d - \psi_{q0} \Delta I_{Ld} - I_{d0} \Delta \psi_q \quad (3.37)$$

(3.36) the speed equation can be written as follows:

$$\frac{d(\omega)}{dt} = \frac{\omega_0}{2H} \Delta T_m - \frac{\omega_0}{2H} (\Delta T_e) - \frac{\omega_0 K_D}{2H} \Delta \omega \quad (3.38)$$

Replacing (3.37) in (3.38), (3.39) can be obtained.

$$\begin{aligned} \frac{d(\omega)}{dt} = & \frac{\omega_0}{2H} \Delta T_m - \frac{\omega_0 \psi_{d0}}{2H} \Delta I_{Lq} + \frac{\omega_0 V_{t0}}{2H X_C} (\psi_{d0} \cos \delta_0 + \psi_{q0} \sin \delta_0) \Delta \delta + \\ & \frac{\omega_0}{2H X_C} (\psi_{d0} \sin \delta_0 + \psi_{q0} \cos \delta_0) \Delta V_t - \frac{\omega_0 I_{q0}}{2H} \Delta \psi_d + \frac{\omega_0 \psi_{q0}}{2H} \Delta I_{Ld} + \\ & \frac{\omega_0 I_{d0}}{2H} \Delta \psi_q - \frac{\omega_0 K_D}{2H} \Delta \omega \end{aligned} \quad (3.39)$$

Arranging linearized (3.31)-(3.39) in matrix form, the following equation can be obtained

$$\left[\frac{d(\Delta X)}{dt} \right] = [A][\Delta X] + [B][\Delta I] + [C][\Delta V_t] + [D][\Delta T_m] \quad (3.40)$$

where

[I] is the current matrix

[T_m] is the external prime mover torque matrix

[V_t] is the variable voltage matrix

[X] is the state variable matrix

$$[\Delta X] = \begin{bmatrix} \Delta \psi_d \\ \Delta \psi_{kd1} \\ \Delta \psi_q \\ \Delta \psi_{kq1} \\ \Delta \delta \\ \Delta \omega \end{bmatrix}$$

$$[\Delta I] = \begin{bmatrix} \Delta I_{Ld} \\ \Delta I_{kd1} \\ \Delta I_{Lq} \\ \Delta I_{kq1} \end{bmatrix}$$

[A], [B], [C] and [D] are matrices consisting of machine parameters and initial operating condition of order 6x6, 6x4, 6x1 and 6x1 respectively as given below.

$$[A] = \begin{bmatrix} 0 & 0 & \omega_o & 0 & \omega_o V_{t0} \left(\cos \delta_o - \frac{R_a}{X_C} \sin \delta_o \right) & \psi_{qo} \\ 0 & 0 & 0 & 0 & 0 & 0 \\ -\omega_o & 0 & 0 & 0 & -\omega_o V_{t0} \left(\sin \delta_o + \frac{R_a}{X_C} \cos \delta_o \right) & -\psi_{do} \\ 0 & 0 & 0 & 0 & 0 & 0 \\ 0 & 0 & 0 & 0 & 0 & 1 \\ \frac{-\omega_o I_{qo}}{2H} & 0 & \frac{\omega_o I_{do}}{2H} & 0 & \frac{\omega_o V_{t0}}{2HX_C} (\psi_{do} \cos \delta_o - \psi_{qo} \sin \delta_o) & \frac{-\omega_o K_D}{2H} \end{bmatrix}$$

$$[B] = \begin{bmatrix} \omega_o R_a & 0 & 0 & 0 \\ 0 & -\omega_o R_{kd1} & 0 & 0 \\ 0 & 0 & \omega_o R_a & 0 \\ 0 & 0 & 0 & -\omega_o R_{kq1} \\ 0 & 0 & 0 & 0 \\ \frac{\omega_o \psi_{qo}}{2H} & 0 & -\frac{\omega_o \psi_{do}}{2H} & 0 \end{bmatrix}$$

$$[C] = \begin{bmatrix} \omega_0 \left(\sin \delta_0 + \frac{R_a}{X_c} \cos \delta_0 \right) \\ 0 \\ \omega_0 \left(\cos \delta_0 - \frac{R_a}{X_c} \sin \delta_0 \right) \\ 0 \\ 0 \\ \frac{\omega_0}{2HX_c} (\psi_{d0} \sin \delta_0 + \psi_{q0} \cos \delta_0) \end{bmatrix}$$

$$[D] = \begin{bmatrix} 0 \\ 0 \\ 0 \\ 0 \\ 0 \\ \frac{\omega_0}{2H} \end{bmatrix}$$

3.3 Stator and Rotor Flux-Linkages Equations

The stator and rotor winding flux linkages can be expressed in terms of machine currents and reactances as follows:

$$\psi_d = -(X_{m ds} + X_l)I_d + X_{m ds}I_{kd1} \quad (3.41)$$

$$\psi_{kd1} = -X_{m ds}I_d + (X_{m ds} + X_{kd1})I_{kd1} \quad (3.42)$$

$$\psi_q = -(X_{m qs} + X_l)I_q + X_{m qs}I_{kq1} \quad (3.43)$$

$$\psi_{kq1} = -X_{m qs}I_q + (X_{m qs} + X_{kq1})I_{kq1} \quad (3.44)$$

Saturation is considered in the direct axis only, so the d-axis magnetizing reactance varies with the corresponding ampere-turns.

Linearizing (3.41)-(3.44), (3.45)-(3.48) can be obtained.

$$\Delta\psi_d = -(X_{m ds0} + X_l)\Delta I_d + X_{m ds0}\Delta I_{kd1} - (I_{d0} - I_{kd10})\Delta X_{m ds} \quad (3.45)$$

$$\Delta\psi_{kd1} = -(X_{m ds0})\Delta I_d + (X_{m ds0} + X_{kd1})\Delta I_{kd1} - (I_{d0} - I_{kd10})\Delta X_{m ds} \quad (3.46)$$

$$\Delta\psi_q = -(X_{m qs0} + X_l)\Delta I_q + X_{m qs0}\Delta I_{kq1} - (I_{q0} - I_{kq10})\Delta X_{m qs} \quad (3.47)$$

$$\Delta\psi_{kq1} = -(X_{mqs0})\Delta I_q + (X_{mqs0} + X_{kq1})\Delta I_{kq1} - (I_{q0} - I_{kq10})\Delta X_{mqs} \quad (3.48)$$

Re-written (3.45)-(3.48) in matrix form.

$$[\Delta\psi] = [X_s][\Delta I_T] + [I_0] \begin{bmatrix} \Delta X_{mds} \\ \Delta X_{mqs} \end{bmatrix} \quad (3.49)$$

Where $[X_s]$ is a 4x4 matrix of generator reactances, $[I_0]$ is a 4x2 matrix that consists of initial values of current.

$$[X_s] = \begin{bmatrix} -(X_{mds0} + X_l) & X_{mds0} & 0 & 0 \\ -X_{mds0} & -(X_{mds0} + X_{kd1}) & 0 & 0 \\ 0 & 0 & -(X_{mqs0} + X_l) & X_{mqs0} \\ 0 & 0 & -X_{mqs0} & (X_{mqs0} + X_{kq1}) \end{bmatrix}$$

$$[I_0] = \begin{bmatrix} -(I_{d0} - I_{kd10}) & 0 \\ -(I_{d0} - I_{kd10}) & 0 \\ 0 & -(I_{q0} - I_{kq10}) \\ 0 & -(I_{q0} - I_{kq10}) \end{bmatrix}$$

3.4 Saturation Characteristics

The accurate prediction of synchronous reluctance generator steady-state behavior requires the proper representation of saturation in the machine modeling. The saturated value of d-axis magnetizing reactance is calculated by modifying the unsaturated value (X_{mdu}) with a saturation factor S_d , calculated from polynomials fitting the saturation curves. The d-axis magnetizing ampere-turns (AT_d) are used to locate the operating point on the saturation characteristics. In this proposed model, saturation in the direct axis has been taken into account by considering a saturation factor S_d .

$$X_{mds} = S_b X_{mdu} \quad (3.50)$$

Linearizing (3.50), (3.51) can be obtained.

$$\Delta X_{mds} = X_{mdu} \Delta S_d \quad (3.51)$$

Using the d-axis saturation characteristic, S_d can be represented in polynomial form as a function of their respective excitation as follows:

$$S_d = D_1 AT_d^4 + D_2 AT_d^3 + D_3 AT_d^2 + D_4 AT_d + D_5 \quad (3.52)$$

Applying a method of linearization to (3.52).

$$\Delta S_d = (4D_1 AT_{d0}^3 + 3D_2 AT_{d0}^2 + 2D_3 AT_{d0} + D_4) \Delta AT_d \quad (3.53)$$

Where D_i is constants for $i = 1, 2, \dots, 5$

$$\Delta S_d = K_{ds} \Delta AT_d \quad (3.54)$$

$$K_{ds} = 4D_1 AT_{d0}^3 + 3D_2 AT_{d0}^2 + 2D_3 AT_{d0} + D_4$$

Parameter K_{ds} depend on the initial values of d-axis ampere-turns.

In per unit system ampere-turns in d-axis can be represented as follows:

$$|AT_d| = |-I_d + I_{kd1}| \quad (3.55)$$

Applying linearization

$$\begin{aligned} |\Delta AT_d| &= |-\Delta I_d + \Delta I_{kd1}| \\ \Delta AT_d &= -(\Delta I_d - \Delta I_{kd1}) \end{aligned} \quad (3.56)$$

Replacing (3.56) in (3.54), (3.57) can be obtained.

$$\Delta S_d = -K_{ds} (\Delta I_d - \Delta I_{kd1}) \quad (3.57)$$

(3.57) can be re-writing as follows:

$$\Delta X_{m ds} = -K'_{ds} (\Delta I_d - \Delta I_{kd1}) \quad (3.58)$$

Saturation in the d-axis thus can be represented as a function of d-axis currents. So change in d-axis saturated reactance value depends on the d-axis currents and can be expressed as

$$[I_0] \begin{bmatrix} \Delta X_{m ds} \\ \Delta X_{m qs} \end{bmatrix} = [X_k] [\Delta I_T] \quad (3.59)$$

$$[X_k] = \begin{bmatrix} (I_{d0} - I_{kd10})X_{mdu}K'_{ds} & -(I_{d0} - I_{kd10})X_{mdu}K'_{ds} & 0 & 0 \\ (I_{d0} - I_{kd10})X_{mdu}K'_{ds} & -(I_{d0} - I_{kd10})X_{mdu}K'_{ds} & 0 & 0 \\ 0 & 0 & 0 & 0 \\ 0 & 0 & 0 & 0 \end{bmatrix}$$

Where $[X_k]$ is a matrix that consists of initial currents, unsaturated d-axis reactances and parameter K'_{ds} .

3.5 State-Matrix of the System

The state-matrix of the system can be derived by substituting (3.59) in (3.49), (3.60) can be obtained.

$$[\Delta \psi] = [X_S] [\Delta I_T] + [X_k] [\Delta I_T] \quad (3.60)$$

$$[\Delta \psi] = ([X_S] + [X_k]) [\Delta I_T] \quad (3.61)$$

(3.60) can be re-written as:

$$[\Delta \psi] = [X_R] [\Delta I_T] \quad (3.62)$$

$$\text{Where } [X_R] = [X_S] + [X_k]$$

As the flux matrix is a sub-set of the state variable matrix, (3.62) can be re-written as:

$$[\Delta X] = [X_R] [\Delta I_T] \quad (3.63)$$

$$[\Delta I_T] = [X_R]^{-1} [\Delta X] \quad (3.64)$$

Using the current matrix (3.23) in (3.64), (3.65) can be obtained.

$$[\Delta I] = [X_R]^{-1} [\Delta X] + [\Delta I_C] \quad (3.65)$$

Replacing (3.65) in (3.40), (3.66) can be obtained.

$$\left[\frac{d(\Delta X)}{dt} \right] = [A] [\Delta X] + [B] \left\{ [X_R]^{-1} [\Delta X] + [\Delta I_C] \right\} + [C] [\Delta V_i] + [D] [\Delta T_m] \quad (3.66)$$

$$\left[\frac{d(\Delta X)}{dt} \right] = ([A] + [B] [X_R]^{-1}) [\Delta X] + [B] [\Delta I_C] + [C] [\Delta V_i] + [D] [\Delta T_m] \quad (3.67)$$

$$\begin{aligned}
[B][\Delta I_c] &= \begin{bmatrix} \frac{\omega_0 R_a V_{i0}}{X_C} \sin \delta_0 \\ 0 \\ \frac{\omega_0 R_a V_{i0}}{X_C} \cos \delta_0 \\ 0 \\ 0 \\ \frac{\omega_0 V_{i0}}{2HX_C} (\psi_{q0} \sin \delta_0 - \psi_{d0} \cos \delta_0) \end{bmatrix} [\Delta \delta] + \begin{bmatrix} \frac{\omega_0 R_a}{X_C} \cos \delta_0 \\ 0 \\ \frac{\omega_0 R_{kq1}}{X_C} \sin \delta_0 \\ 0 \\ 0 \\ \frac{\omega_0 \psi_{q0}}{2HX_C} \cos \delta_0 \end{bmatrix} [\Delta V_t] \\
[B][\Delta I_c] &= \begin{bmatrix} 0 & 0 & 0 & 0 & \frac{\omega_0 R_a V_{i0}}{X_C} \sin \delta_0 & 0 \\ 0 & 0 & 0 & 0 & 0 & 0 \\ 0 & 0 & 0 & 0 & \frac{\omega_0 R_a V_{i0}}{X_C} \cos \delta_0 & 0 \\ 0 & 0 & 0 & 0 & 0 & 0 \\ 0 & 0 & 0 & 0 & 0 & 0 \\ 0 & 0 & 0 & 0 & 0 & 0 \\ 0 & 0 & 0 & 0 & \frac{\omega_0 V_{i0}}{2HX_C} (\psi_{q0} \sin \delta_0 - \psi_{d0} \cos \delta_0) & 0 \end{bmatrix} [\Delta X] + \begin{bmatrix} \frac{\omega_0 R_a}{X_C} \cos \delta_0 \\ 0 \\ \frac{\omega_0 R_{kq1}}{X_C} \sin \delta_0 \\ 0 \\ 0 \\ 0 \\ \frac{\omega_0 \psi_{q0}}{2HX_C} \cos \delta_0 \end{bmatrix} [\Delta V_t]
\end{aligned}$$

$$[B][\Delta I_c] = [Y][\Delta X] + [G][\Delta V_t] \quad (3.68)$$

(3.68) can be re-written by replacing the capacitor current matrix by the state variable matrix, (3.69) can be obtained.

$$\begin{aligned}
\left[\frac{d(\Delta X)}{dt} \right] &= ([A] + [B][X_R]^{-1})[\Delta X] + [Y][\Delta X] + [G][\Delta V_t] + [C][\Delta V_t] + [D][\Delta T_m] \\
\left[\frac{d(\Delta X)}{dt} \right] &= ([A] + [B][X_R]^{-1} + [Y])[\Delta X] + \{[G] + [C]\}[\Delta V_t] + [D][\Delta T_m] \quad (3.69)
\end{aligned}$$

$$\left[\frac{d(\Delta X)}{dt} \right] = [P][\Delta X] + [J][\Delta V_t] + [D][\Delta T_m] \quad (3.70)$$

The matrix $[P]$ is the state matrix of the developed machine model for stand-alone operation.

3.6 Calculation of the Elements of the State Matrix

From (3.70), $[P]$ can be written as:

$$[P] = [A] + [B][X_R]^{-1} + [Y] \quad (3.71)$$

Suppose

$$[Z] = [A] + [Y] \quad (3.72)$$

where

$$[Z] = \begin{bmatrix} 0 & 0 & \omega_0 & 0 & \omega_0 V_{t0} \cos \delta_0 & \psi_{q0} \\ 0 & 0 & 0 & 0 & 0 & 0 \\ -\omega_0 & 0 & 0 & 0 & -\omega_0 V_{t0} \sin \delta_0 & -\psi_{d0} \\ 0 & 0 & 0 & 0 & 0 & 0 \\ 0 & 0 & 0 & 0 & 0 & 1 \\ \frac{-\omega_0 I_{q0}}{2H} & 0 & \frac{\omega_0 I_{d0}}{2H} & 0 & 0 & \frac{-\omega_0 K_D}{2H} \end{bmatrix}$$

Using (3.71) in (3.70)

$$[P] = [Z] + [B][X_R]^{-1}$$

where

$$[X_R] = [X_S] + [X_k]$$

$$[X_R] = \begin{bmatrix} x_{11} & x_{12} & x_{13} & x_{14} \\ x_{21} & x_{22} & x_{23} & x_{24} \\ x_{31} & x_{32} & x_{33} & x_{34} \\ x_{41} & x_{42} & x_{43} & x_{44} \end{bmatrix}$$

$$x_{11} = -(X_{m ds 0} + X_l) + I_{d0} X_{m du} K_{ds}$$

$$x_{12} = X_{m ds 0} - I_{d0} X_{m du} K_{ds}$$

$$x_{21} = -X_{m ds 0} + I_{d0} X_{m du} K_{ds}$$

$$x_{22} = (X_{m ds 0} + X_{kd1}) - I_{d0} X_{m du} K_{ds}$$

$$x_{33} = -(X_{m qs 0} + X_l)$$

$$x_{34} = X_{m qs 0}$$

$$x_{43} = -X_{m qs 0}$$

$$x_{44} = X_{m qs 0} + X_{kq1}$$

$$x_{13} = x_{14} = x_{23} = x_{24} = x_{31} = x_{32} = x_{41} = x_{42} = 0$$

Performing matrix inverse on $[X_R]$

Suppose $[R] = [X_R]^{-1}$

$$[R] = \begin{bmatrix} \frac{x_{22}}{x_{11}x_{22} - x_{12}x_{21}} & \frac{-x_{12}}{x_{11}x_{22} - x_{12}x_{21}} & 0 & 0 \\ \frac{-x_{21}}{x_{11}x_{22} - x_{12}x_{21}} & \frac{x_{11}}{x_{11}x_{22} - x_{12}x_{21}} & 0 & 0 \\ 0 & 0 & \frac{x_{44}}{x_{33}x_{44} - x_{34}x_{43}} & \frac{-x_{22}}{x_{33}x_{44} - x_{34}x_{43}} \\ 0 & 0 & \frac{-x_{43}}{x_{33}x_{44} - x_{34}x_{43}} & \frac{x_{22}}{x_{33}x_{44} - x_{34}x_{43}} \end{bmatrix}$$

Using the values of the inversed matrix $[R]$

$$[B][X_R]^{-1} = [B][R] \quad (3.73)$$

$$[B][R] = \begin{bmatrix} \omega_0 R_a R_{11} & \omega_0 R_a R_{12} & 0 & 0 \\ -\omega_0 R_{kd1} R_{21} & -\omega_0 R_{kd1} R_{22} & 0 & 0 \\ 0 & 0 & \omega_0 R_a R_{33} & \omega_0 R_a R_{34} \\ 0 & 0 & -\omega_0 R_{kq1} R_{43} & -\omega_0 R_{kq1} R_{44} \\ 0 & 0 & 0 & 0 \\ \frac{\omega_0 \Psi_{q0} R_{11}}{2H} & \frac{\omega_0 \Psi_{q0} R_{12}}{2H} & \frac{-\omega_0 \Psi_{d0} R_{33}}{2H} & \frac{-\omega_0 \Psi_{d0} R_{34}}{2H} \end{bmatrix}$$

$$[P] = [K] + [B][R] \quad (3.74)$$

$$[P] = \begin{bmatrix} b_{11} & b_{12} & \omega_0 & 0 & \omega_0 V_{i0} \cos \delta_0 & \Psi_{q0} \\ b_{21} & b_{22} & 0 & 0 & 0 & 0 \\ -\omega_0 & 0 & b_{33} & b_{34} & -\omega_0 V_{i0} \sin \delta_0 & -\Psi_{d0} \\ 0 & 0 & b_{43} & b_{44} & 0 & 0 \\ 0 & 0 & 0 & 0 & 0 & 1 \\ b_{61} - \frac{\omega_0 I_{q0}}{2H} & b_{62} & b_{63} + \frac{\omega_0 I_{d0}}{2H} & b_{64} & 0 & \frac{-\omega_0 K_D}{2H} \end{bmatrix} \quad (3.75)$$

Eigenvalue analysis can be performed on the state matrix, $[P]$, to obtain information on the steady-state stability of the system. For the system to be stable, the oscillation should die out with time which is indicated by a negative real part. Positive real part indicates increasing oscillation which leads to instability. The imaginary part indicates the frequency of oscillation. For any stable system, all the eigenvalues obtained must have a negative real part.

3.7 Numerical Analysis

Numerical analysis has been carried out on a 0.37 kW synchronous reluctance generator using the developed model. The machine stator terminals are connected to a capacitor bank for self-excitation. The values of the unsaturated d- and q-axis magnetizing reactances along with the other machine parameters are presented in Table 3.1. An iterative process has been applied to determine the initial values as the machine d-axis magnetizing reactance varies with saturation. The d-axis saturation characteristics of this machine are shown in Fig. 3.3.

Table 3.1
Machine parameters

Machine Parameters	Values
Rated power	0.37 kW
Rated voltage	400 V
Rated speed	3600 rpm
Capacitance	100 μ F
Unsaturated d-axis reactance	1.267 pu
Unsaturated q-axis reactance	0.317 pu
Leakage reactance	0.0317 pu
Armature resistance	0.0392 pu
d-axis damper circuit reactance	1.0 pu
q-axis damper circuit reactance	0.3 pu
d-axis damper circuit resistance	0.03 pu
q-axis damper circuit resistance	0.02 pu
Mechanical inertia	3.795 sec
Damping torque coefficient	0.0

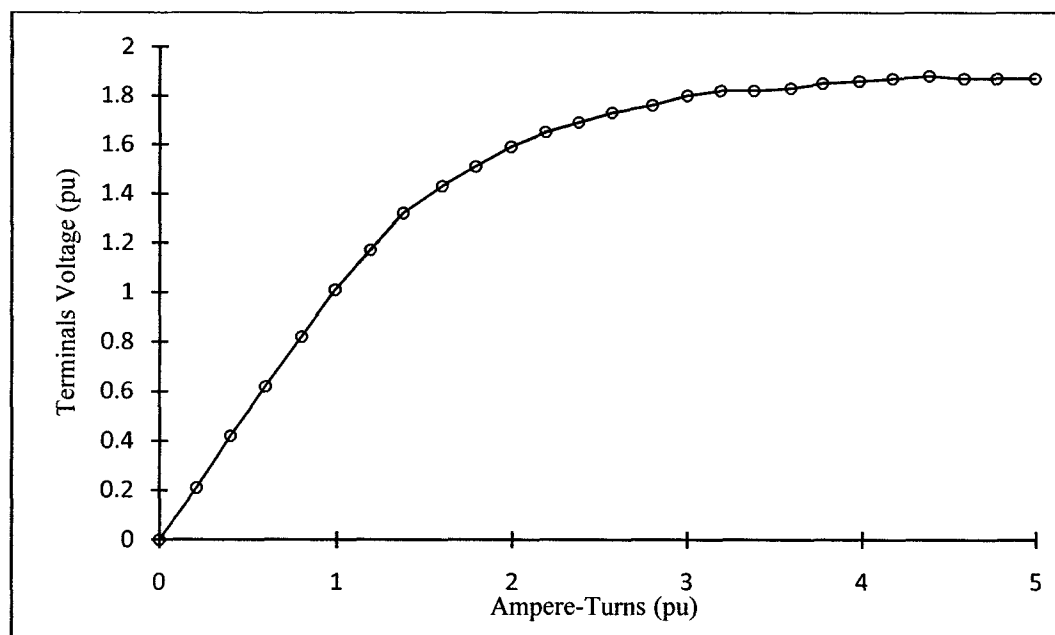


Fig. 3.3. d-axis saturation characteristics.

3.8 Results of Steady-State Analysis

A MATLAB program has been developed to compute the initial values under certain operating conditions as shown in the flow chart in Fig. 3.4. The state matrix of the synchronous reluctance generator has been used to calculate the eigenvalues of the state matrix for different operating conditions. The flowchart in Fig. 3.5 explains the way to calculate eigenvalues from the state-matrix of the system.

A steady-state stability analysis has been performed for different loading conditions. The effect of excitation capacitance has also been looked into; the eigenvalues corresponding to active, reactive and apparent power output have been plotted to investigate the stability status of the synchronous reluctance generator.

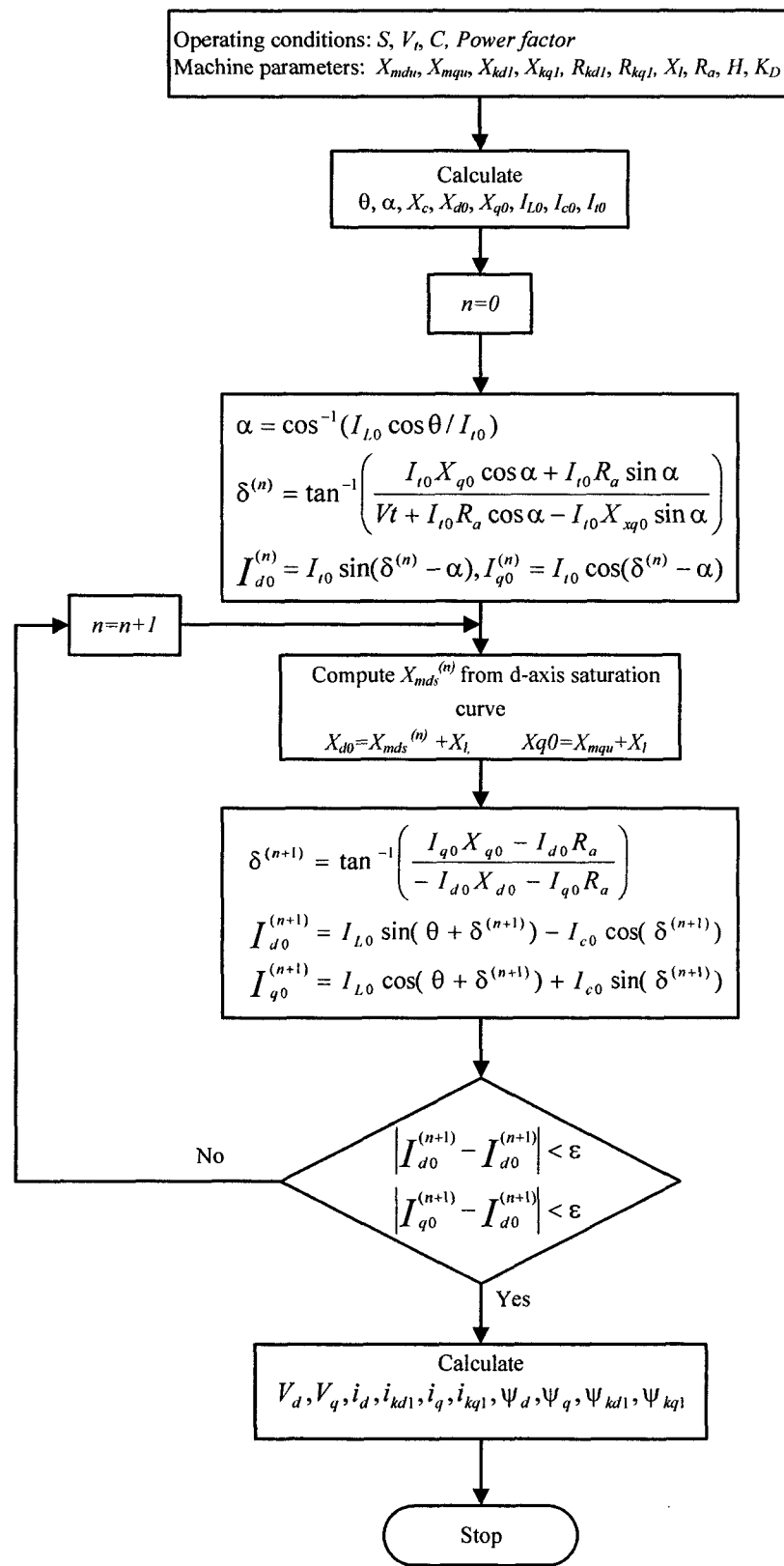


Fig. 3.4. Initial value calculation flow chart for steady-state analysis.

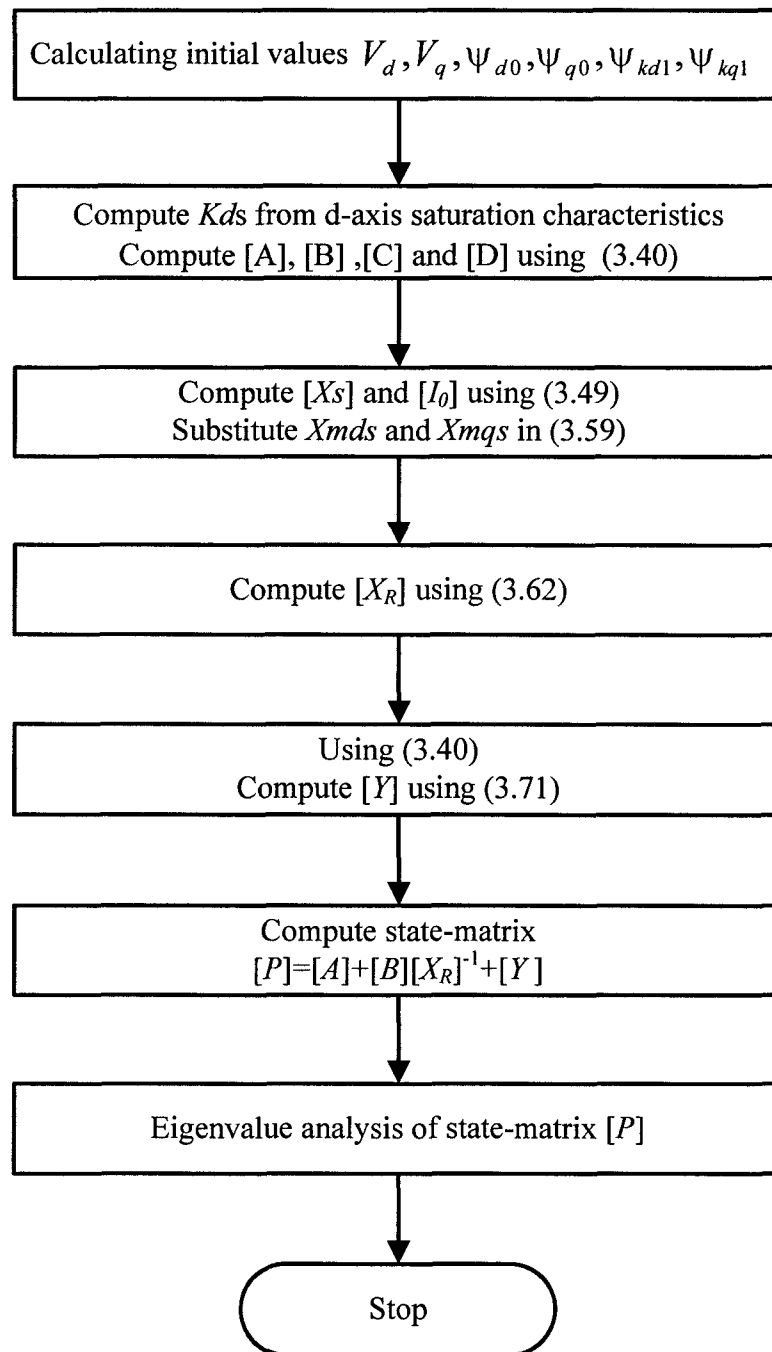


Fig. 3.5. Flow chart for steady-state stability analysis.

Figs. 3.6 and 3.7 show the effect of active and the reactive power on the steady-state stability performance of machine. It can be seen from these figures that with an increase in the active and reactive power output, the system stability decreases. The stability of the system can be realized from the real parts of the eigenvalues.

In Fig. 3.8, the eigenvalues corresponding to different apparent power output are presented. It is observed that with the increase in apparent power output the real parts of eigenvalues become less negative which shows the system moves towards instability. The machine is more stable at lower apparent power output.

In the case of a stand-alone system, the excitation capacitance is a requisite for self-excitation process and also has an effect on steady-state stability of the system. The effect of excitation capacitance on the machine stability is shown in Fig. 3.9. It can be seen that with the increase in the excitation capacitance value, system stability increases.

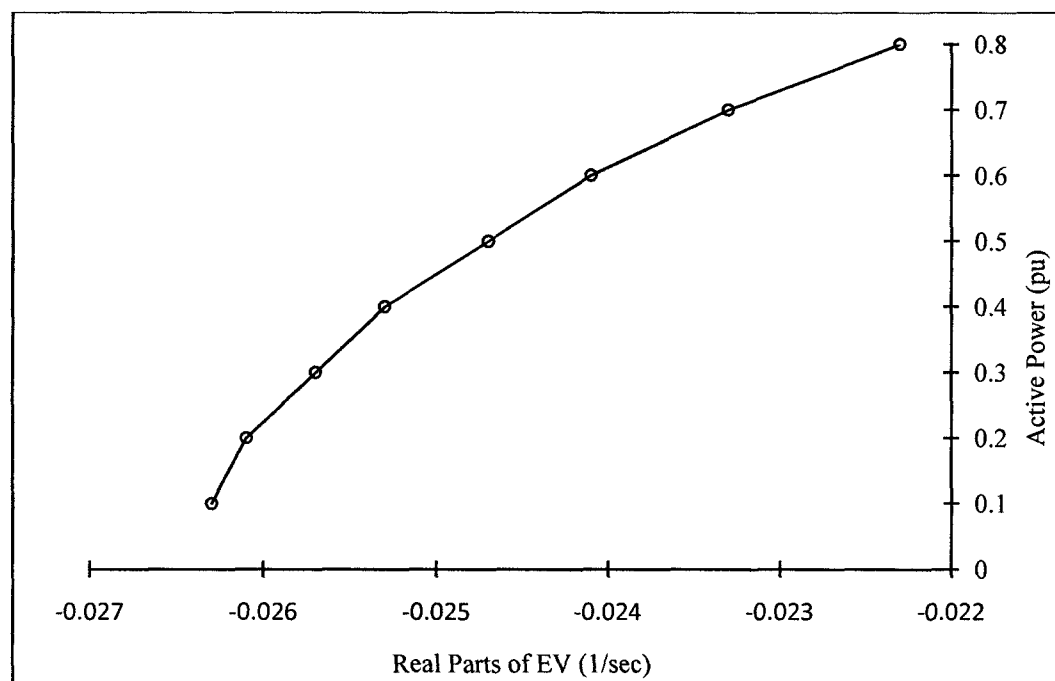


Fig. 3.6. Real parts of eigenvalues corresponding to different active power output for $C=100 \mu\text{F}$ and $Q=0.436 \text{ pu}$.

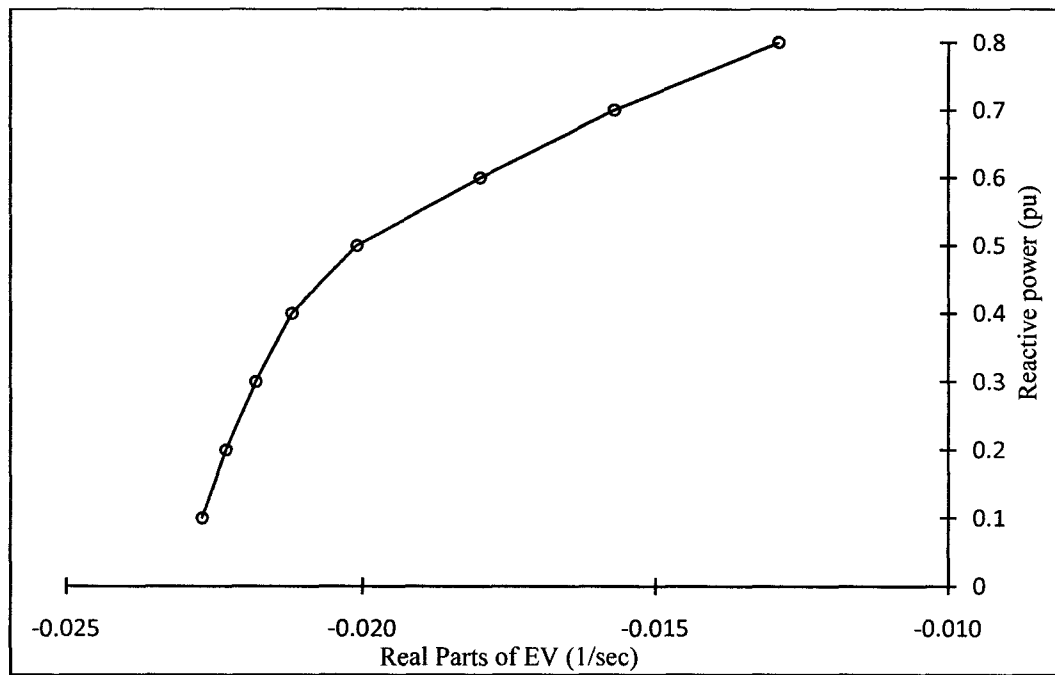


Fig. 3.7. Real parts of eigenvalues corresponding to different reactive power output for $C=100 \mu\text{F}$ and $P=0.900 \text{ pu}$.

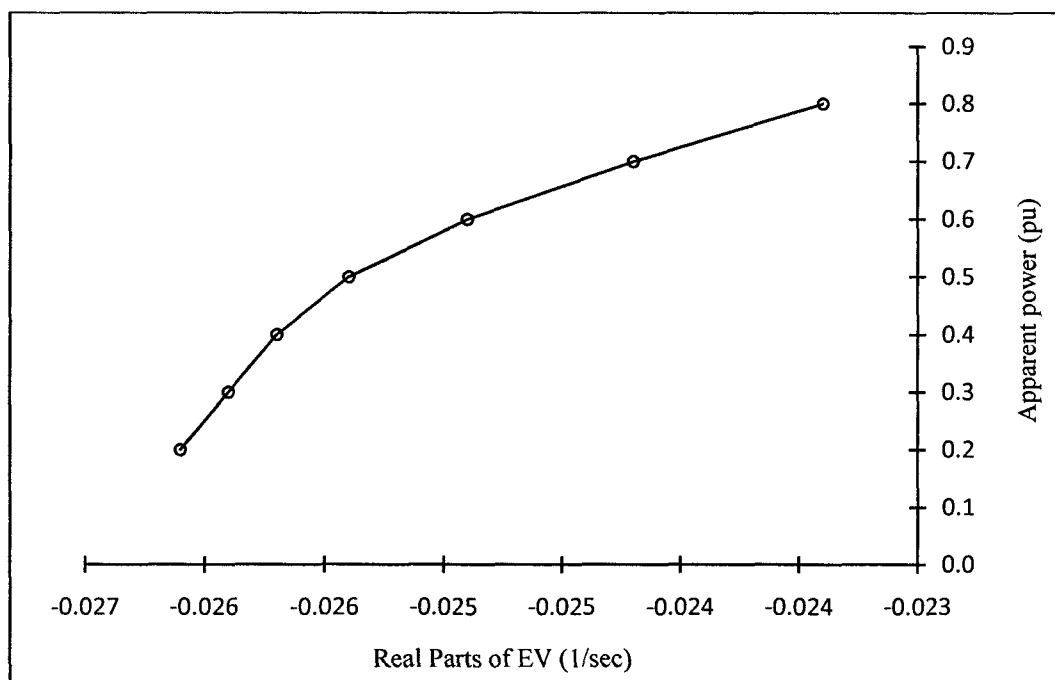


Fig. 3.8. Real parts of eigenvalues corresponding to different apparent power demand.

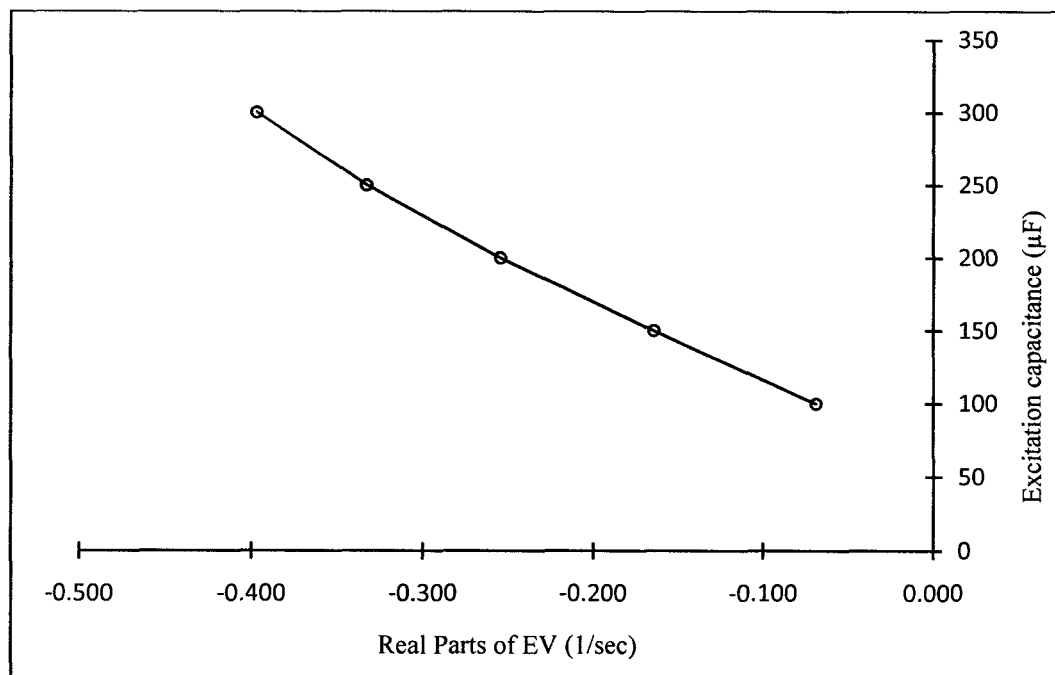


Fig. 3.9. Real parts of eigenvalues corresponding to different excitation capacitance for $P=0.9$ pu and $Q=0.436$ pu.

3.9 Sensitivity Analysis to Steady-State Model

The machine steady-state condition depends upon the circuit parameters; any change in their values may affect the stability of the system. To analyze the effect of machine parameters on the stability condition, circuit parameters have been varied from 50% to 150% of their standard values at different excitation capacitance. Circuit parameters such as R_{kd1} , R_{kq1} , X_{kd1} , X_{kq1} , R_a and X_l have been varied from 50% to 150% of their standard values at excitation capacitance of 100 μF, 125 μF and 150 μF. Eigenvalue sensitivity of machine parameters have been calculated by using state-matrix of the system.

3.10 Results of Sensitivity Analysis

Fig. 3.10 shows the real parts of eigenvalues characteristics for a range of 80% to 110% with a step increase 5% of the standard value (active power output) of the machine. Real parts of eigenvalues (Real part of complex eigen value, Most dominant eigen value,

and 3rd dominant eigen value) have been plotted corresponding to the percentage change in active power at different excitation capacitances. Eigen values sensitivity due to change in active power can be observed from the graph. Similarly, Fig. 3.11 shows the real parts of eigenvalues for a change in the reactive power output from 60% to 140% with a step increase 10% of reactive power at 100 μ F, 125 μ F and 150 μ F excitation capacitance.

Figs. 3.12 to 3.17 show the eigen value sensitivity characteristics for a range of 50% to 150% with a step increase 10% of their standard values for circuit parameters (R_{kd1} , R_{kq1} , X_{kd1} , X_{kq1} , R_a and X_l) at 100 μ F, 125 μ F and 150 μ F excitation capacitance.

Fig. 3.12 and Fig. 3.13 show the real parts of eigenvalues corresponding to percentage change in d-axis damper resistance and q-axis damper circuit resistance at different excitation capacitance respectively. It has been observed that the stability level improves with an increase in the value of d-axis damper circuit resistance and q-axis damper circuit resistance. It has also been found that stability level improves with increase in the values of excitation capacitance.

Fig. 3.14 shows the eigenvalues sensitivity with the change in d-axis damper circuit reactances at different excitation capacitance. It has been analyzed that stability level decreases with the increase in the value of d-axis damper circuit reactance. It has also observed that the stability level increases with the increase in excitation capacitance. Similarly Fig. 3.15 shows that stability level decreases with an increase in the value of q-axis damper circuit reactance and stability level improves with an increase in the value of excitation capacitance. From the investigation of the Fig 3.14 and Fig. 3.15, it has been inferred that 2nd dominant eigenvalues of d-axis damper circuit reactance is more sensitive as compared to the q-axis damper circuit reactance at different excitation capacitance.

Fig. 3.16 and Fig. 3.17 show the real parts of eigenvalues corresponding to the percentage change in armature resistance and leakage reactance at different excitation capacitances respectively. By analyzing these figures, it is observed that there are no significant changes with the increase or decrease in armature resistance and leakage reactance.

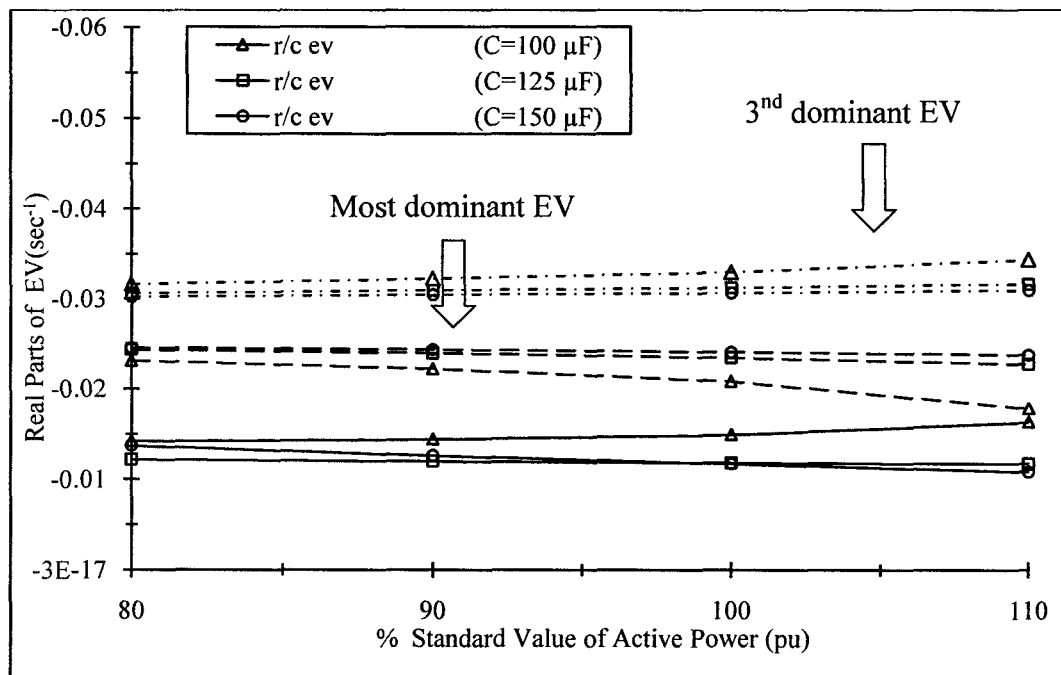


Fig. 3.10. Real parts of eigenvalues corresponding to % change in active power.

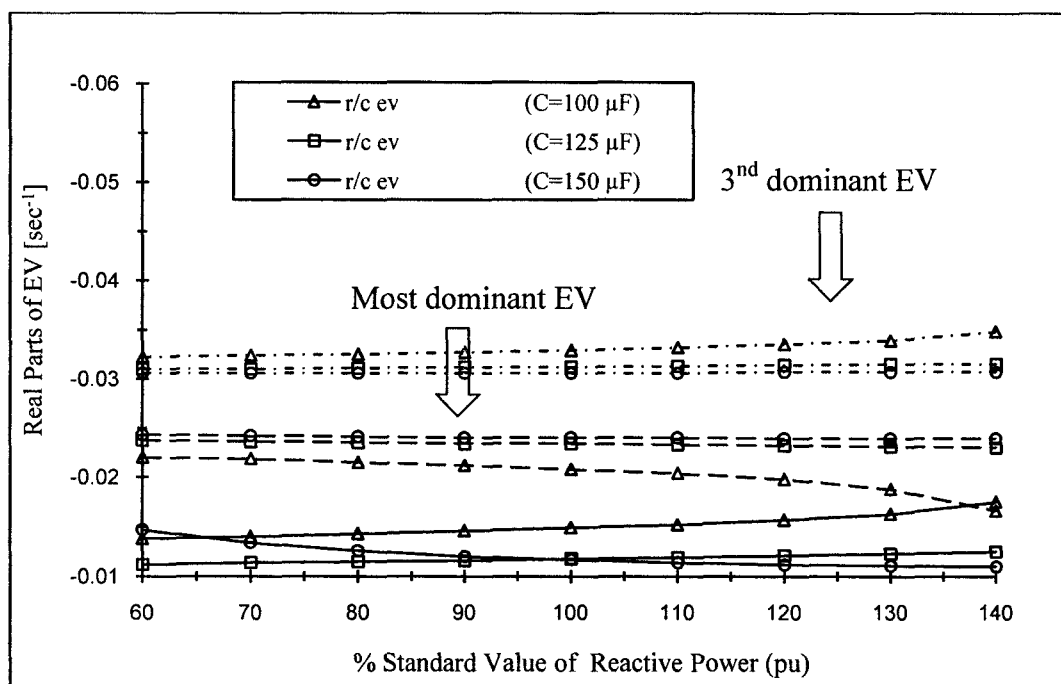


Fig. 3.11. Real parts of eigenvalues corresponding to % change in reactive power.

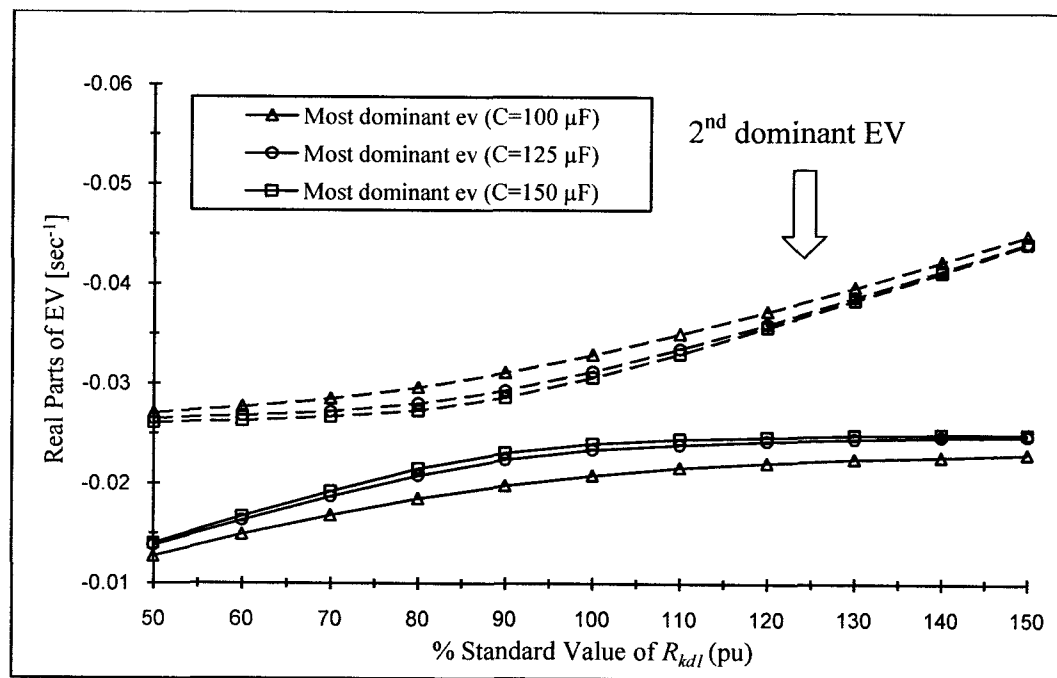


Fig. 3.12. Real parts of eigenvalues corresponding to % change in d-axis damper circuit resistance.

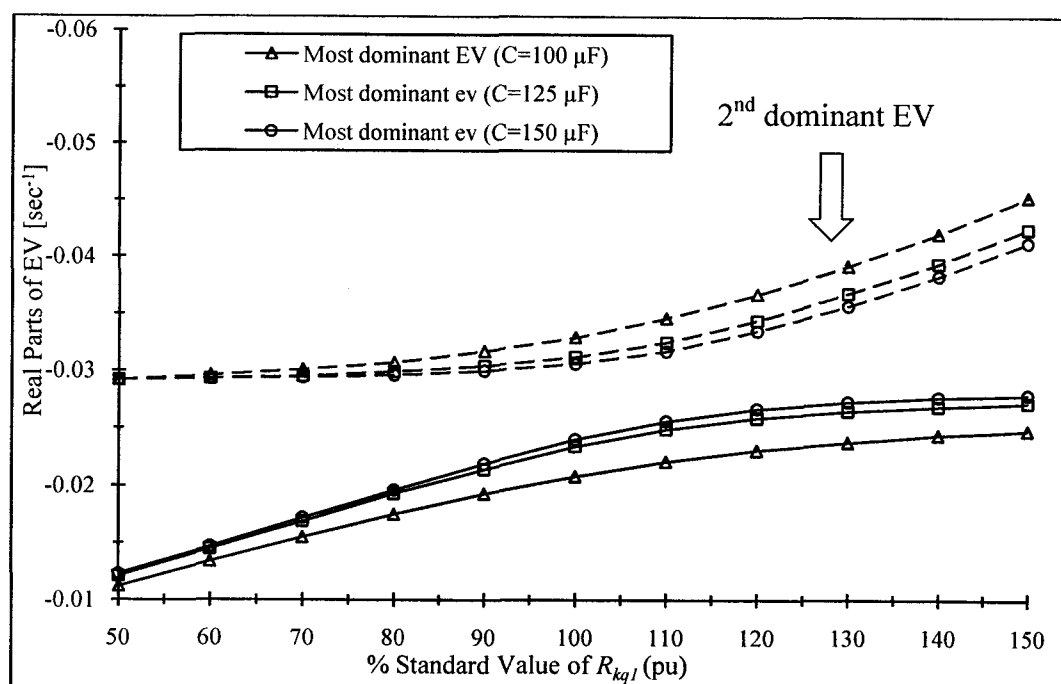


Fig. 3.13. Real parts of eigenvalues corresponding to % change in q-axis damper circuit resistance.

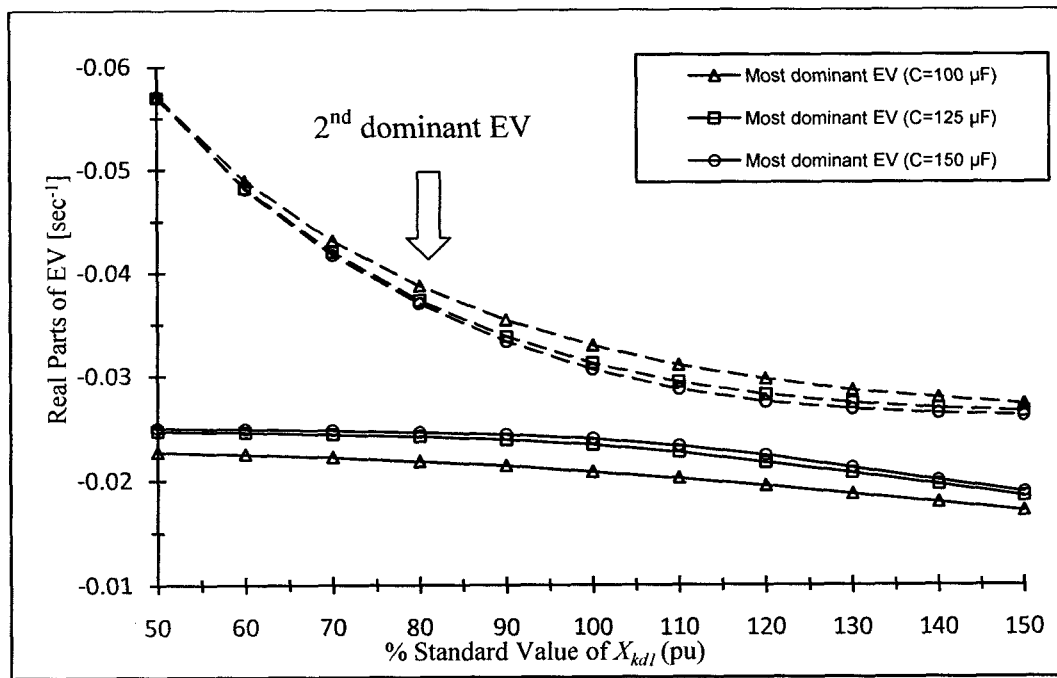


Fig. 3.14. Real parts of eigenvalues corresponding to % change in d-axis damper circuit reactance.

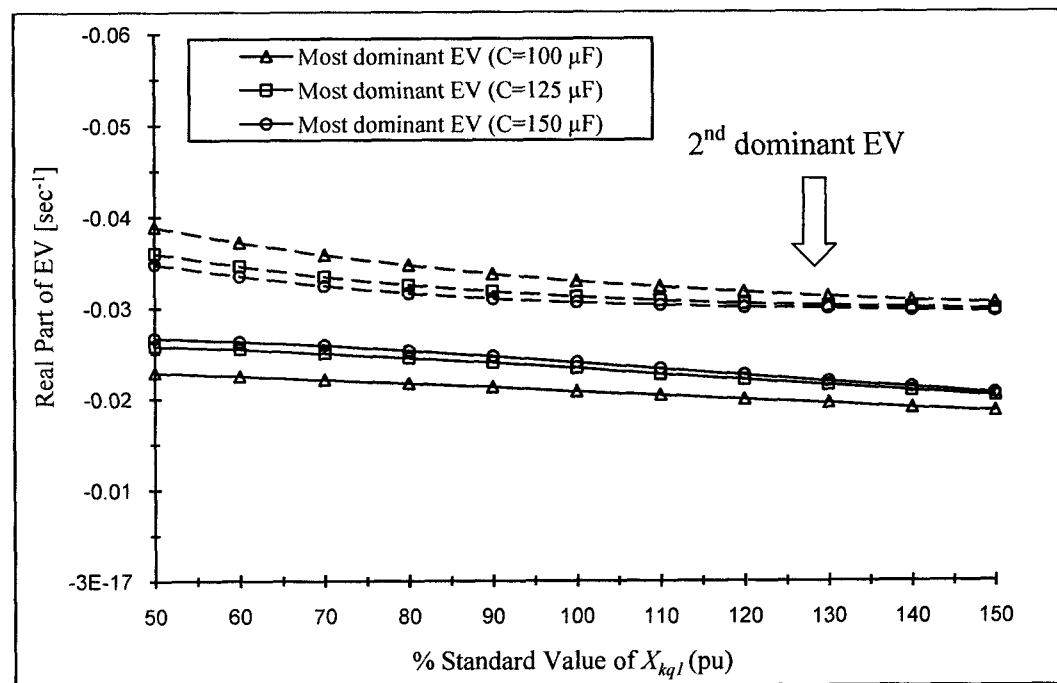


Fig. 3.15. Real parts of eigenvalues corresponding to % change in q-axis damper circuit reactance.

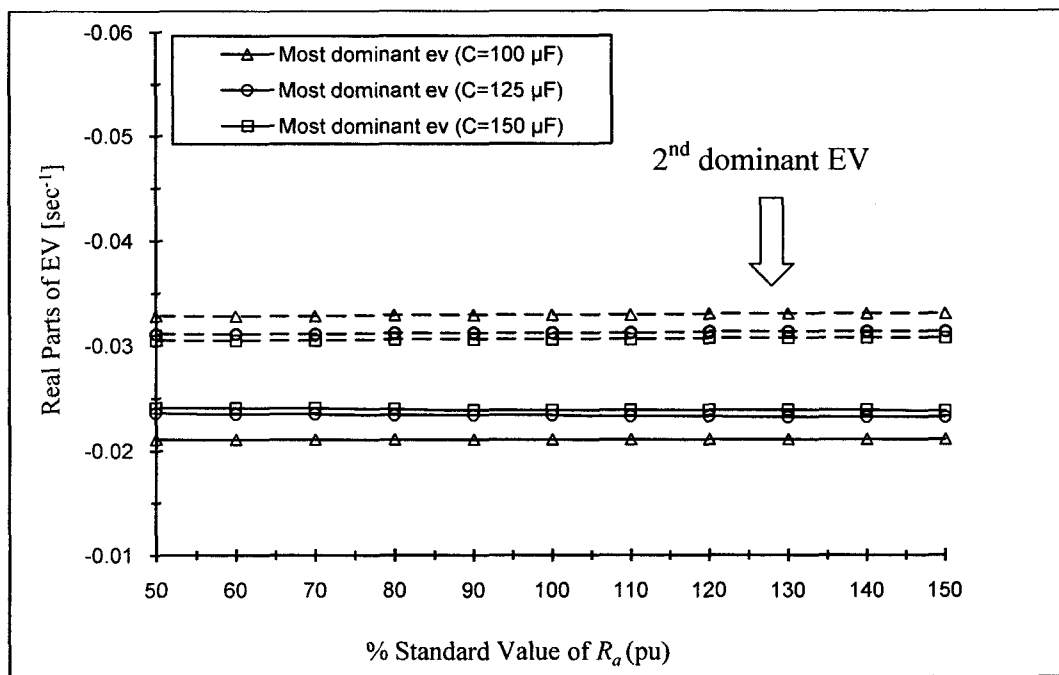


Fig. 3.16. Real part of eigenvalues corresponding to % in armature resistance.

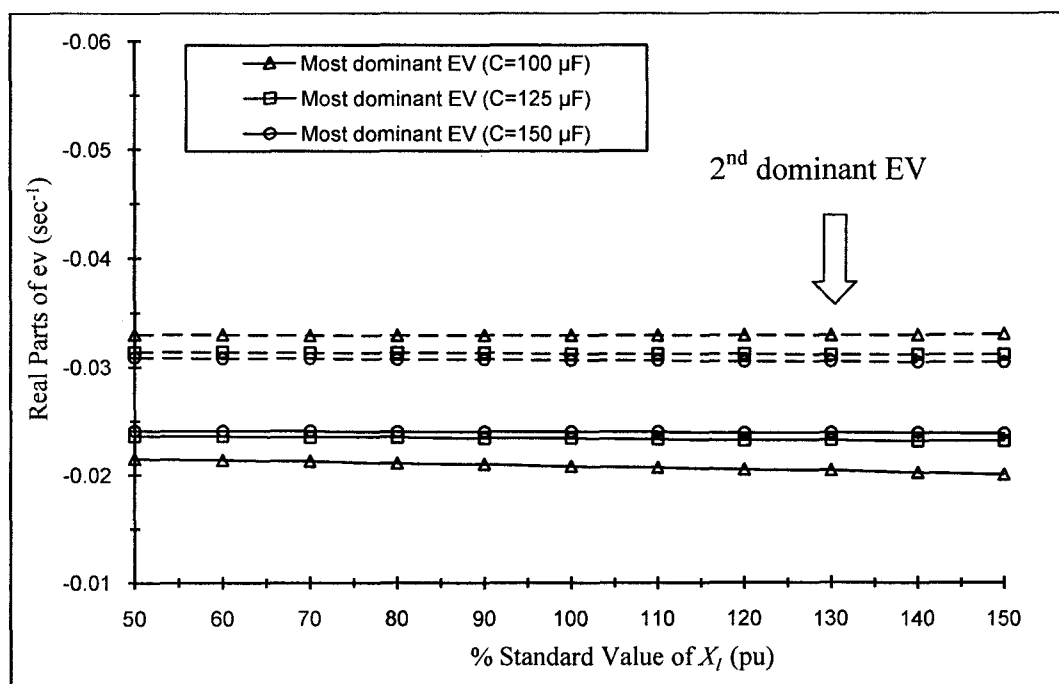


Fig. 3.17. Real parts of eigenvalues corresponding to % change in leakage reactance.

From the eigenvalue sensitivity analysis to steady-state model of self-excited synchronous reluctance generator, it has been found that eigenvalues are most sensitive to d-axis damper circuit reactance as compared to other parameters of the machine. The machine parameters as shown in Table: 3.2 are ranked according to eigenvalue sensitivity.

Table 3.2

Summary of results: Eigen value sensitivity analysis to steady-state model

Machine Parameters (pu)	Average Change in Real Parts of EV(1/sec)
d-axis damper circuit reactance (X_{kdl})	0.01816
d-axis damper circuit resistance (R_{kdl})	0.0143
q-axis damper circuit resistance (R_{kql})	0.01425
q-axis damper circuit reactance (X_{kql})	0.00595
Leakage reactance (X_l)	0.00052
Armature resistance (R_a)	0.0001

3.11 References

- [1] A.L.Mohamadein, Y.H.A. Rahim, A.S. Al-khalaf, "Steady-state performance of a self-excited reluctance generator," *IEE Proceeding on Electric Power Application*, vol.138, pp. 193-198, May 1991.
- [2] S. Ghua and N.C. Kar, "Saturation modeling and stability analysis of synchronous reluctance generator," *IEEE Trans. Energy Conversion*, vol.23, Sep. 2008.
- [3] S. Rana and N.C. Kar, "Steady-state analysis of self-excited synchronous reluctance generator," presented at the *2008 IEEE Canadian Conference on Electrical & Computer Engineering*, Niagara Falls, and May.
- [4] N.C. Kar and J. Tamura, "Effects of synchronous machine saturation, circuit parameters, and control systems on steady-state stability," *Electric Machines and Power Systems*, pp. 327-342, 1999.

4 TRANSIENT ANALYSIS

4.1 Transient Model

A transient model for a self-excited synchronous reluctance generator has been developed considering one damper winding on the direct axis and one damper winding on the quadrature axis. The effect of saturation is also considered in the direct axis while investigating the transient performance of the machine.

The assumptions made in the development of machine model are as follow:

- Core and stray losses are neglected.
- The effect of mutual coupling on d- and q-axis is neglected.
- q-axis saturation is ignored.

There are two methods for integration of differential equations in a power system simulation, one is an explicit method, such as the 4th order Runge-Kutta method, and the other is an implicit method, such as the trapezoidal rule. In this research work, the 4th order Runge-Kutta method has been used to calculate the transient performance of a self-excited reluctance generator. The initial values of the machine parameters have been calculated for a given operating condition using the flow chart shown in Fig. 3.4.

To investigate the transient performance of a three-phase, 0.37 kW, 2-pole, 400 V self-excited synchronous reluctance generator, a three-phase symmetrical short-circuit fault is applied across the machine terminals. At the initiation of the fault, the terminal voltage becomes zero. The corresponding machine differential equations i.e. stator and rotor voltage equations, (3.24) - (3.27), mechanical equations, (3.28) - (3.29), and electromagnetic torque equation, (3.30), are solved to calculate the values of the fluxes, currents, load angle, speed and electromagnetic torque in each time step. In each time step, a 4th order Runge-Kutta method has been employed to solve differential equations using the coefficients of the Runge-Kutta method and the value of parameters obtained from the previous time step. The newly obtained values have been used as the initial values for the next time step. When the fault is cleared, the terminal voltage regains its original value.

A software program has been developed in MATLAB to carry out the transient analysis and the corresponding flow chart diagram has been presented in Fig. 4.1. The

differential equations are solved to obtain currents taking the saturation effect into account. The currents obtained are then compared and the process is repeated until the error is minimized.

The calculated currents, flux linkages, speed and load angle at the end of each time step can be used in order to find the transient performance for the next time step. Table 4.1 shows the simulation parameters of the machine.

Table 4.1
Simulation parameters

Machine Parameters (pu)	Ratings
Terminal voltage	1 pu
Active power	0.9 pu
Reactive Power	0.436 pu
Simulation time	2 sec
Short-circuit fault time	0.05 sec
Fault clearance time	0.05 sec
Time step	0.0005 sec

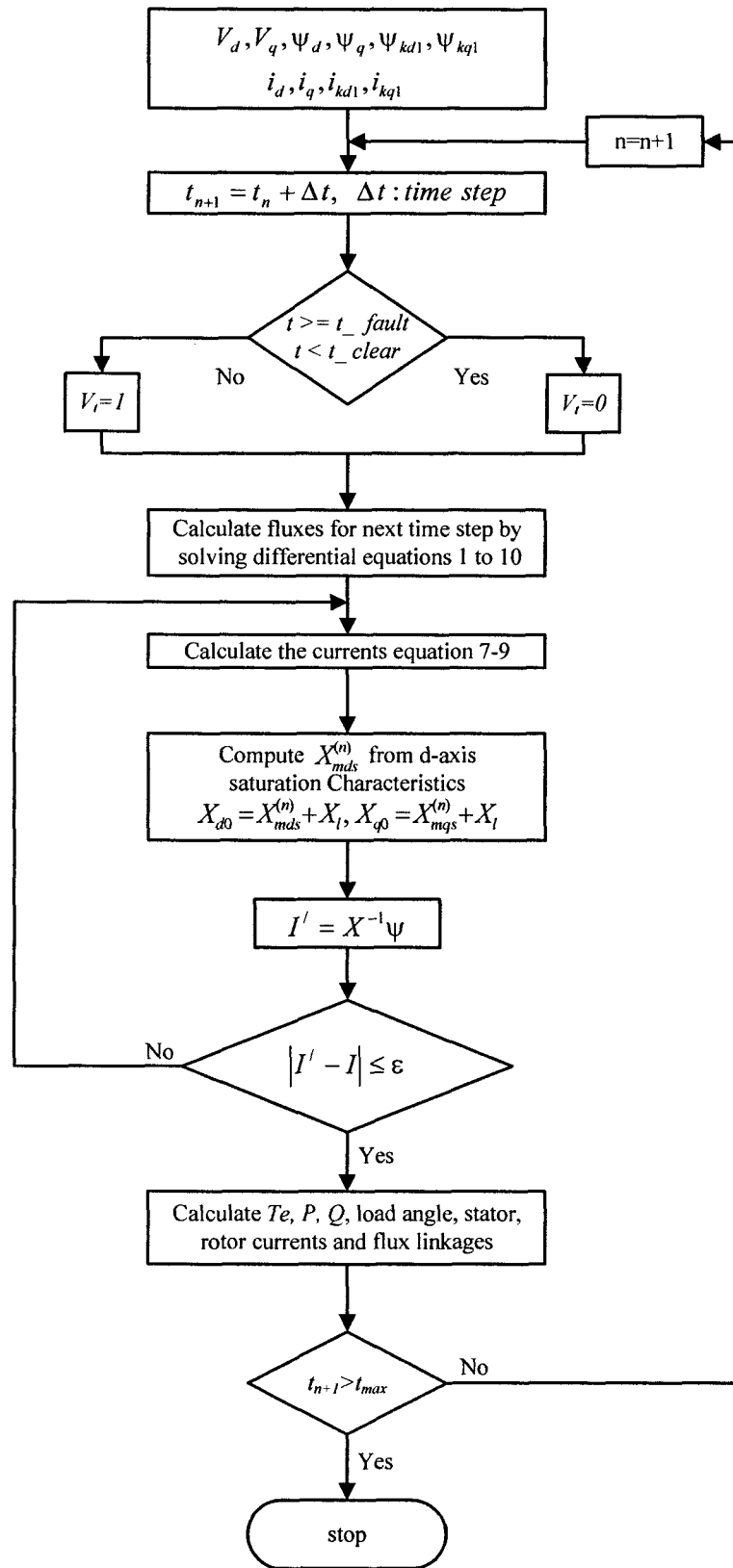


Fig. 4.1. Transient analysis calculation flowchart.

4.2 Transient Stability Analysis Results

Transient analysis has been performed for a three-phase symmetrical short-circuit fault across the terminals of the self-excited synchronous reluctance generator by considering saturation in the direct axis. Variations in the load angle, speed, and electromagnetic torque, stator and rotor currents, stator and rotor flux linkages and active and reactive power have been investigated. The fault was initiated at time 0.05 second and was cleared after 0.05 second.

Fig. 4.2 shows the variation of the load angle of the generator. It can be seen from this figure that there are oscillations after the fault is initiated. Once the fault is cleared, the load angle returns to its original value of around 1.5 second. Fig. 4.3 shows the oscillation in the generator speed. When the fault is cleared, the speed of the generator comes back to its original value after some oscillations. Similarly, Fig. 4.4 shows the transient variation of the electromagnetic torque.

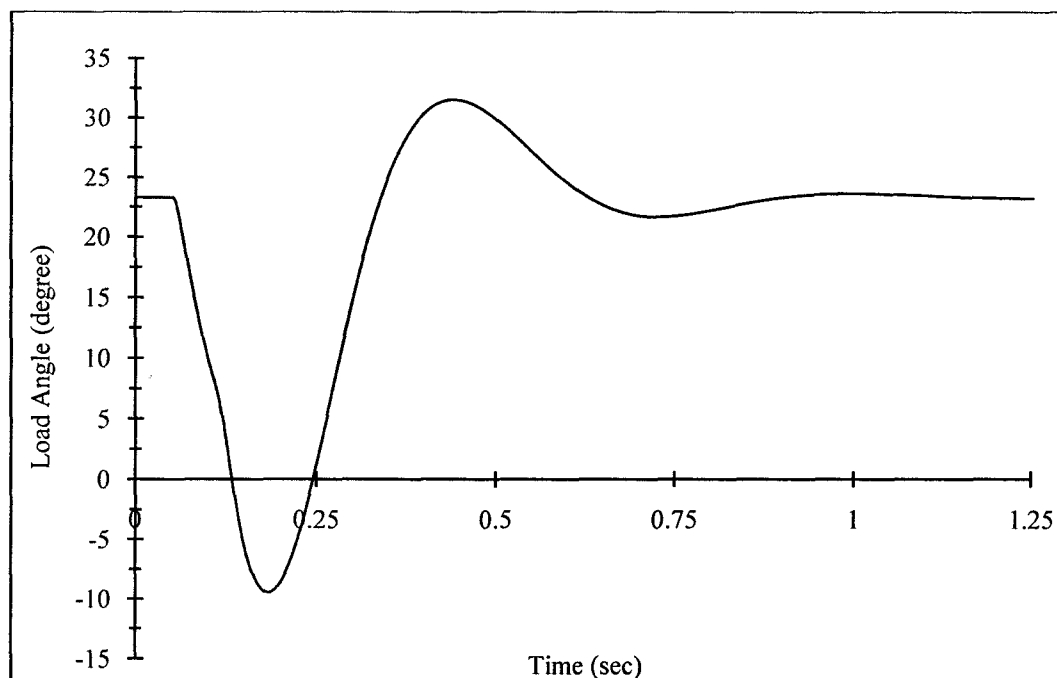


Fig. 4.2. Transient variation of load angle.

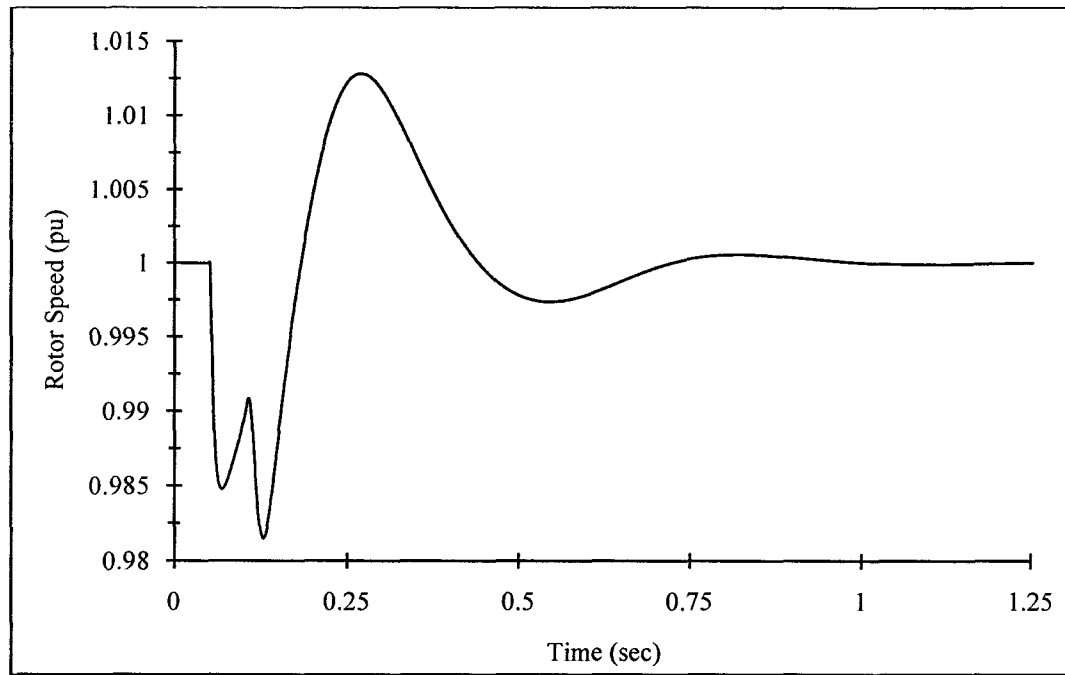


Fig. 4.3. Transient variation of rotor speed.

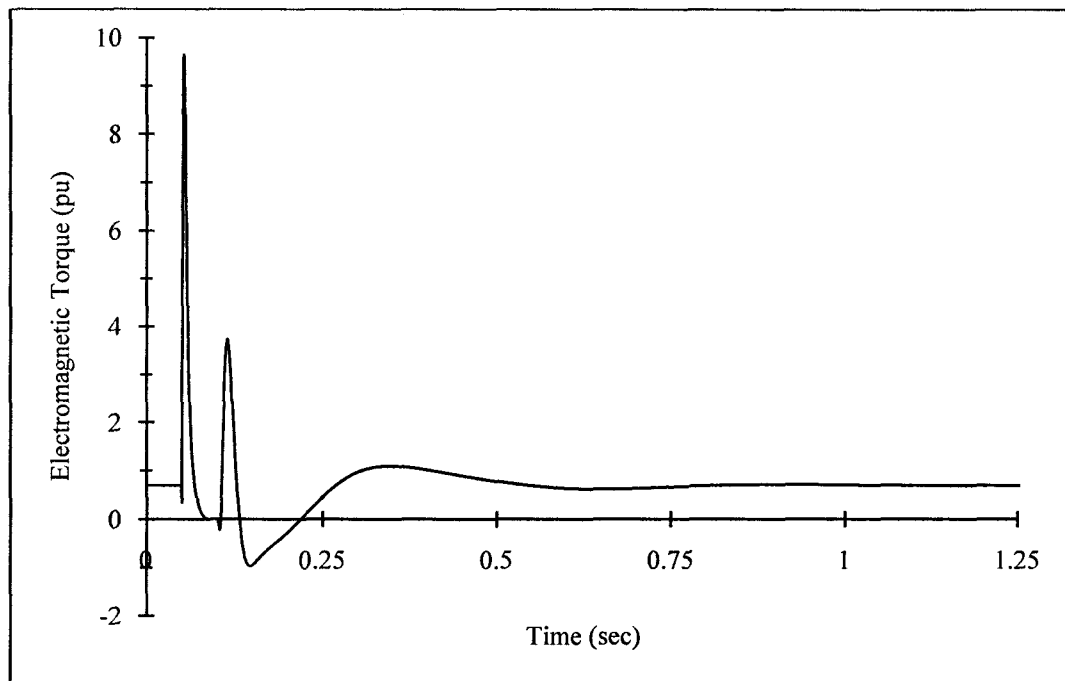


Fig. 4.4. Transient variation of electromagnetic torque.

The oscillations in the d-axis and q-axis stator currents have been shown in Figs. 4.5 and 4.6. They return to their original values after the fault is cleared. Transient variations in the d- and q-axis damper circuit currents have also been shown in Figs. 4.7 and 4.8. The variation in the d-axis and q-axis stator flux-linkages has been shown in Fig.4.9 and Fig. 4.10, respectively. After the fault is cleared, the stator flux linkages return to their original values. Similarly, the rotor flux linkages have been shown in Fig. 4.11 and Fig. 4.12. It can be seen from these figures that the rotor flux linkages become zero after the fault is cleared.

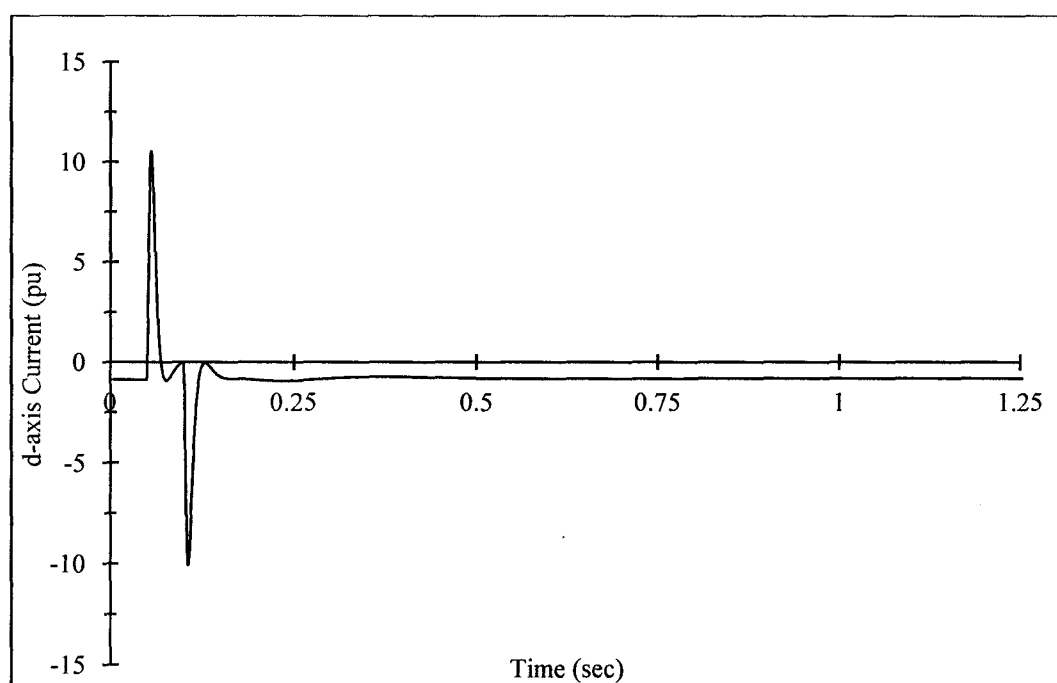


Fig. 4.5. Transient variation of d-axis current.

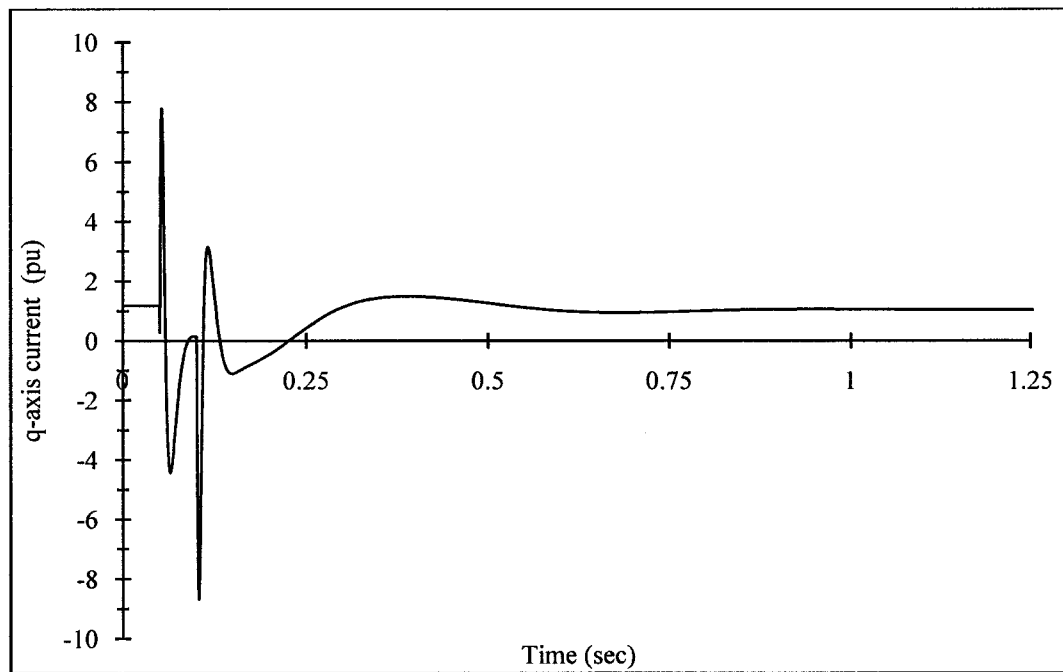


Fig. 4.6. Transient variation of q-axis current.

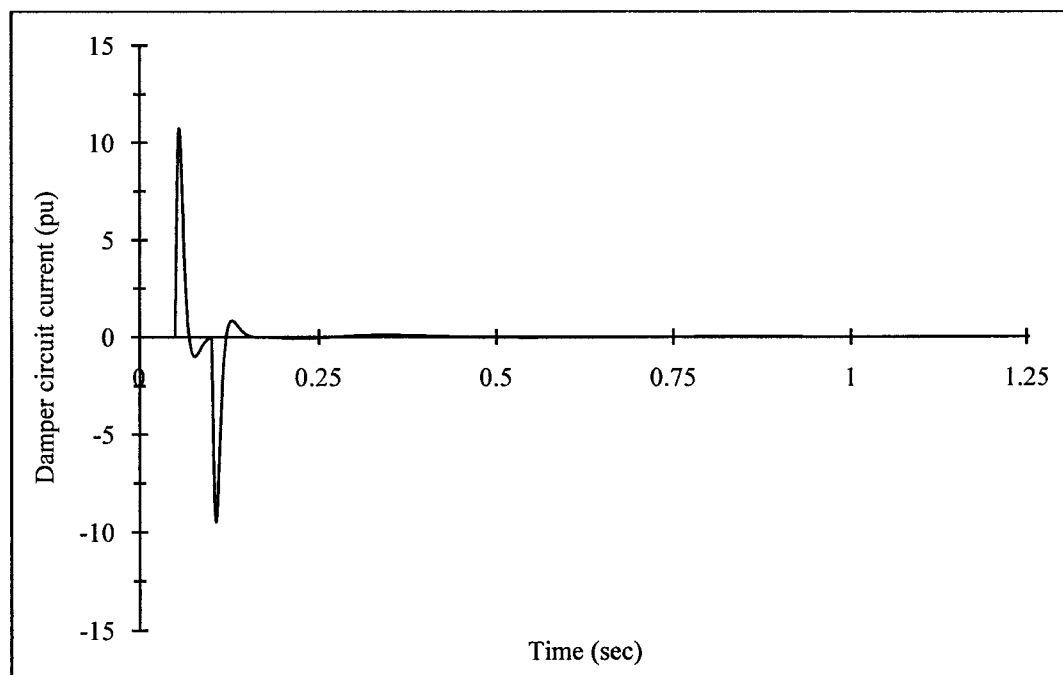


Fig. 4.7. Transient variation d-axis damper circuit current.

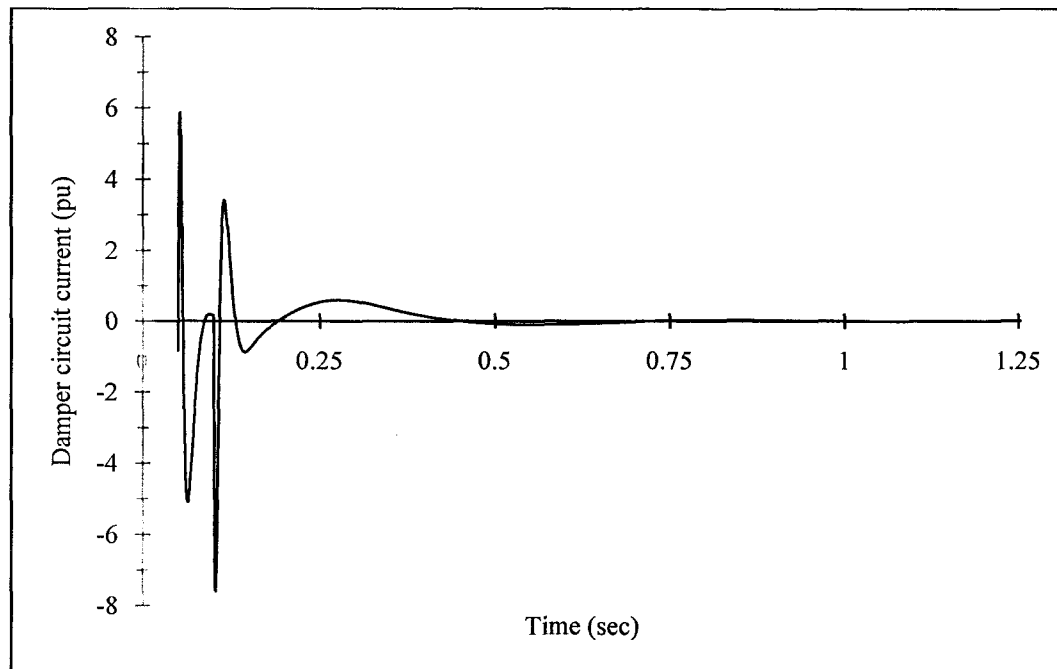


Fig. 4.8. Transient variation q-axis damper circuit current.

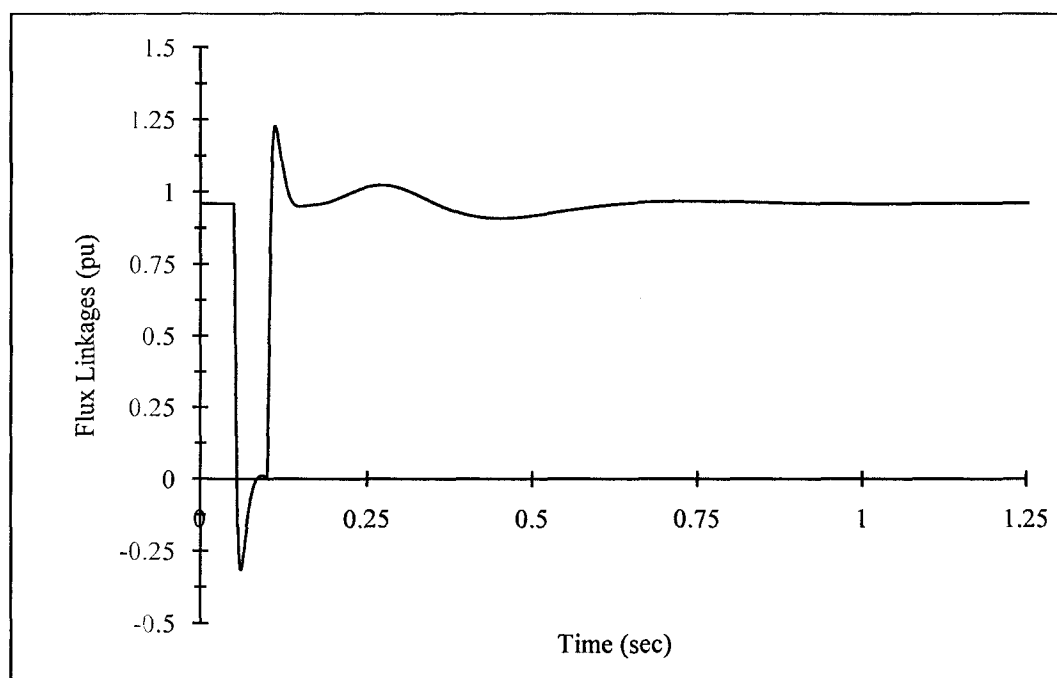


Fig. 4.9. Transient variation of d-axis flux linkage.

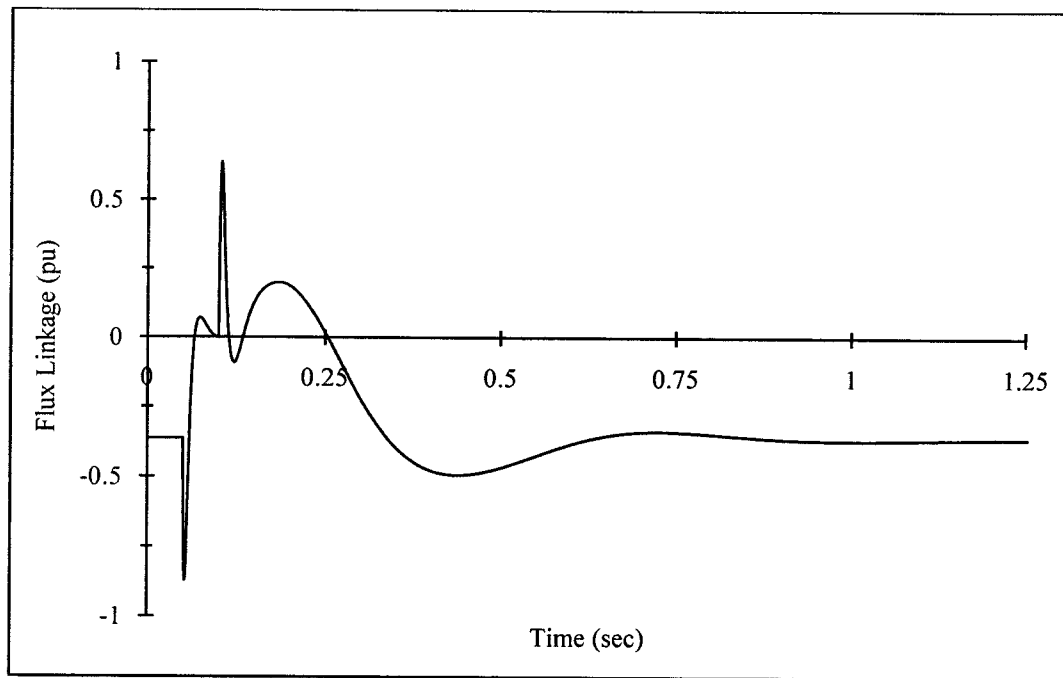


Fig. 4.10. Transient variation q-axis flux linkage.

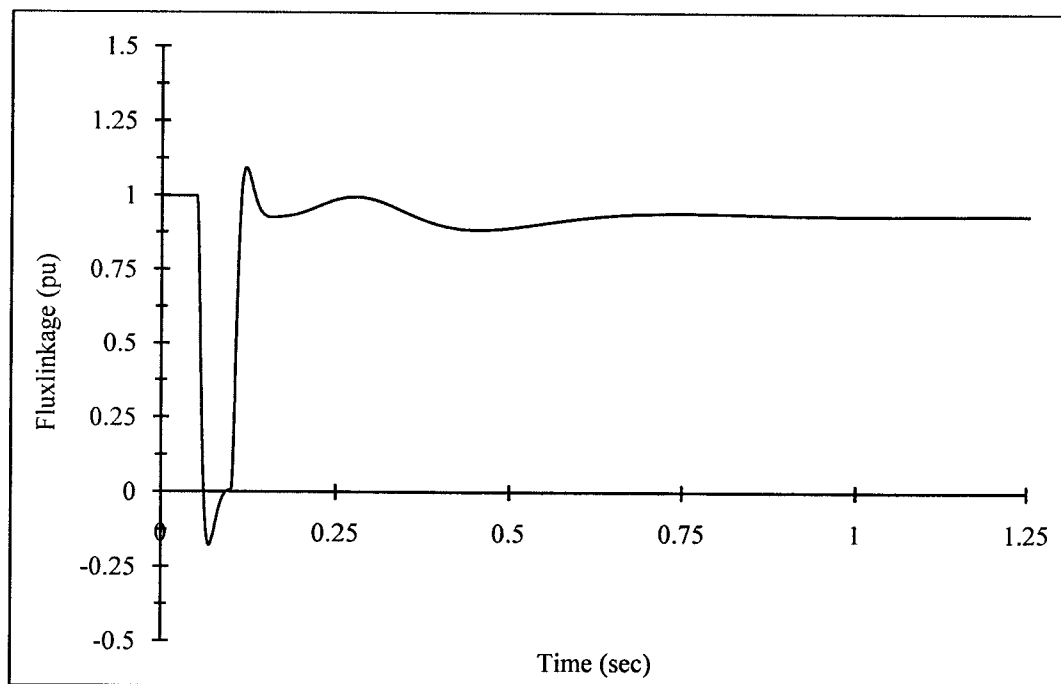


Fig. 4.11. Transient variation of d-axis damper circuit flux linkage.

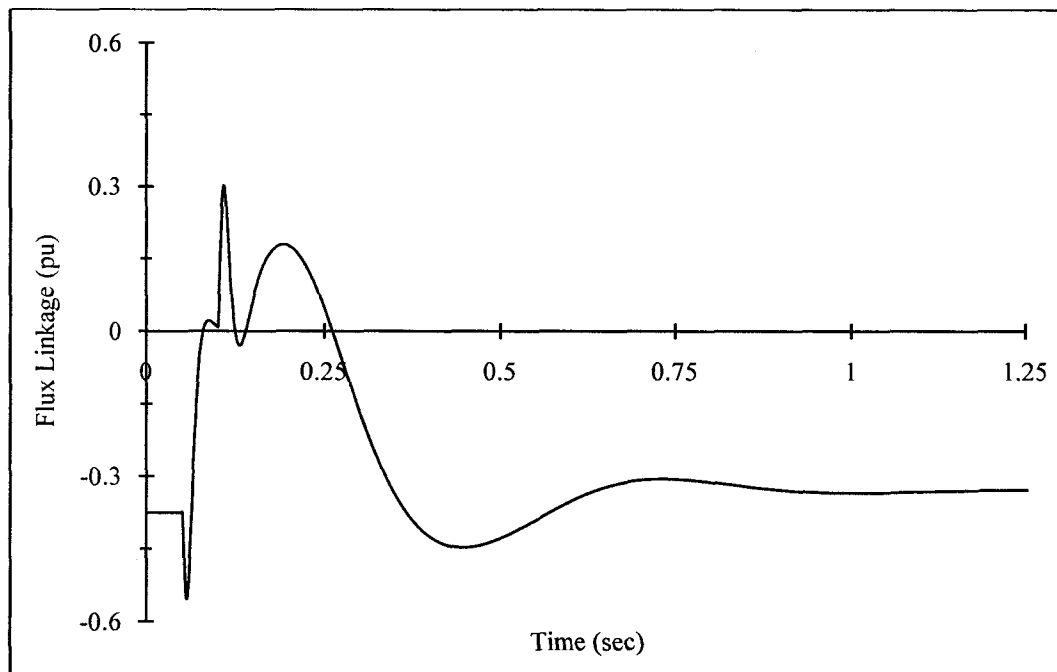


Fig. 4.12. Transient variation of q-axis damper circuit flux linkage.

The machine was subjected to longer fault duration in order to investigate the machine transient stability performance. The fault was applied across the machine terminals for different durations ranging from 0.05 sec to 0.3 sec. It has been observed that after the fault is cleared the machine returns to the original steady-state operating condition for fault duration up to 0.25 sec. When the fault duration is 0.3 sec, the machine lost its synchronism. It is observed that the generator is marginally stable for fault duration of 0.28 sec and becomes unstable for fault duration of 0.29 sec. Fig. 4.13 shows three different scenarios for the stable, marginally stable and unstable cases, respectively.

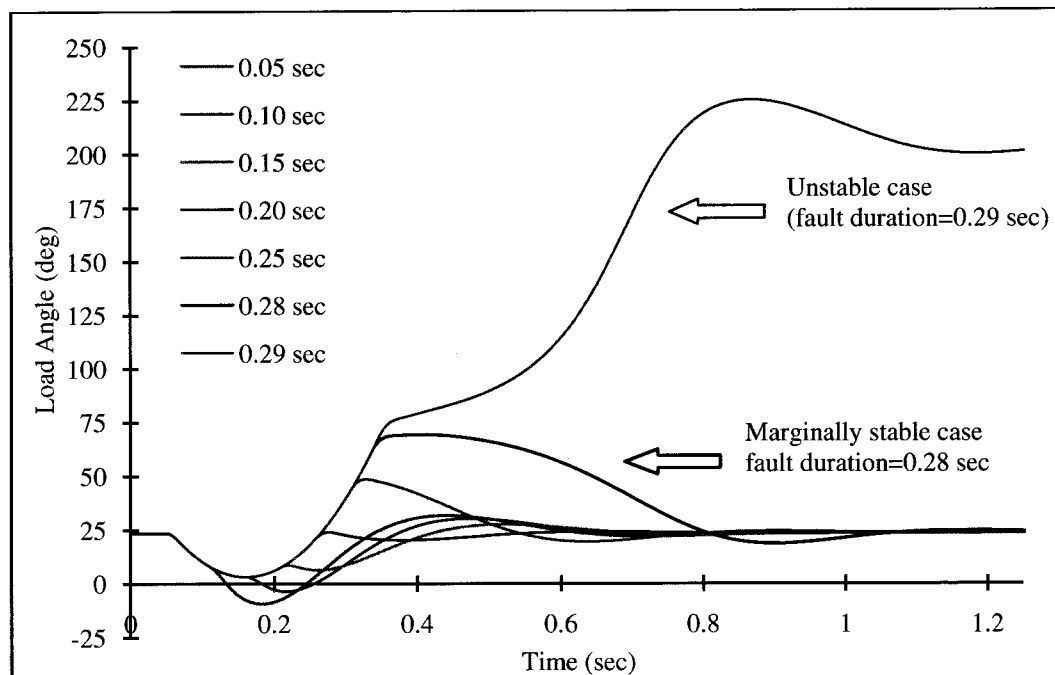


Fig. 4.13. Load angle swing corresponding to different fault durations.

Table: 4.2
Load angle swing for longer fault durations

Fault duration (sec)	Load Angle (deg)	Status
0.05-0.25	28° (Avg.)	stable
0.28	48°	Marginally stable
0.29	220°	Unstable

The critical clearing time has been found to be 0.28 sec by considering the saturation on the direct axis. From the analysis it has been observed that longer fault duration has considerable effect which should be kept in mind during the machine design. Table 4.2 shows the load angle variation and the three different operating regions of the machine against different fault duration.

4.3 Sensitivity Analysis to Transient Model

The machine circuit parameters have been varied from 50%, 75%, 100%, 125% & 150% of their standard values. A capacitor bank of 100 μF is connected across the stator terminals of generator for self-excitation. Load angle swing for different machine parameters (R_{kd1} , R_{kq1} , X_{kd1} , X_{kq1} , R_a and X_l) have been analyzed by using the proposed transient model of self-excited synchronous reluctance generator. Load angle sensitivity for machine parameters have been analyzed for fault duration of 0.05 sec.

4.4 Results of Sensitivity Analysis

Figs. 4.14 to 4.17 show the load angle swing for a range of 50% to 150% with a step increase of 25% of their standard values for circuit parameters R_{kd1} , R_{kq1} , X_{kd1} , X_{kq1} , R_a and X_l at 100 μF excitation capacitance.

Fig. 4.14 and Fig. 4.15 show load angle swing for different d-axis and q-axis damper circuit resistances respectively. From these figures, it has been found that with the increase in d- and q-axis damper circuit resistance, the load angle swing increases. It has also observed that the q-axis damper circuit resistance causes more oscillation in the load angle after fault is cleared as compared to that of d-axis damper circuit resistance.

Fig. 4.16 and Fig. 4.17 show the load angle swing for different d- and q-axis damper circuit reactances. It has been found that stability increases with the increase in d- and q-axis damper circuit resistance.

Fig. 4.18 and Fig.4.19 show the load angle swing for different armature resistance and leakage reactance at 100 μF excitation capacitance.

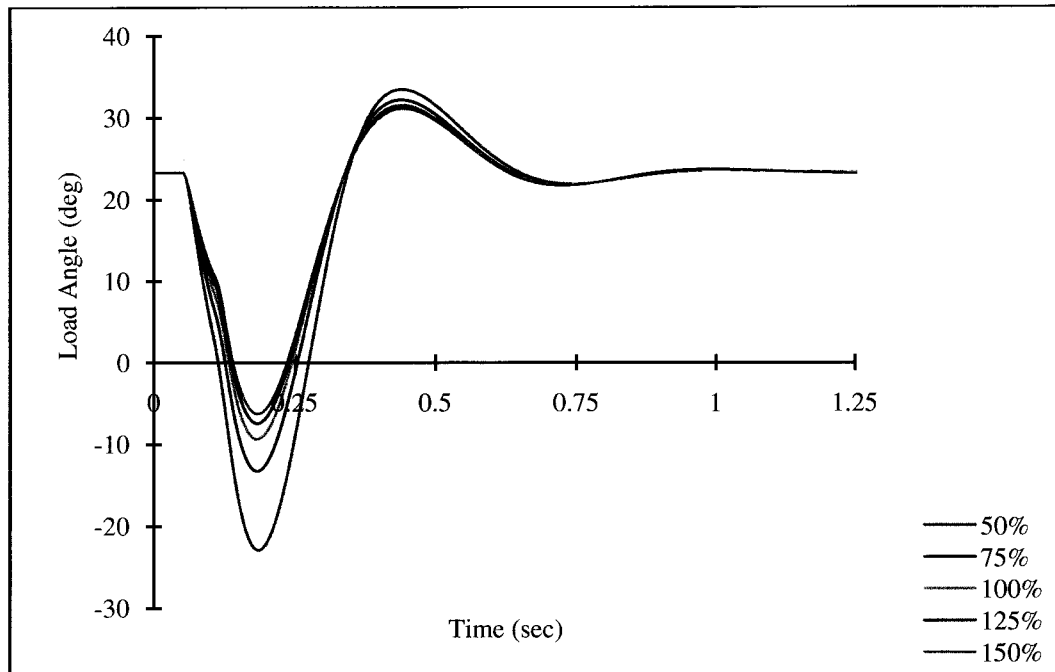


Fig. 4.14. Swing in the load angle for different d-axis damper circuit resistance.

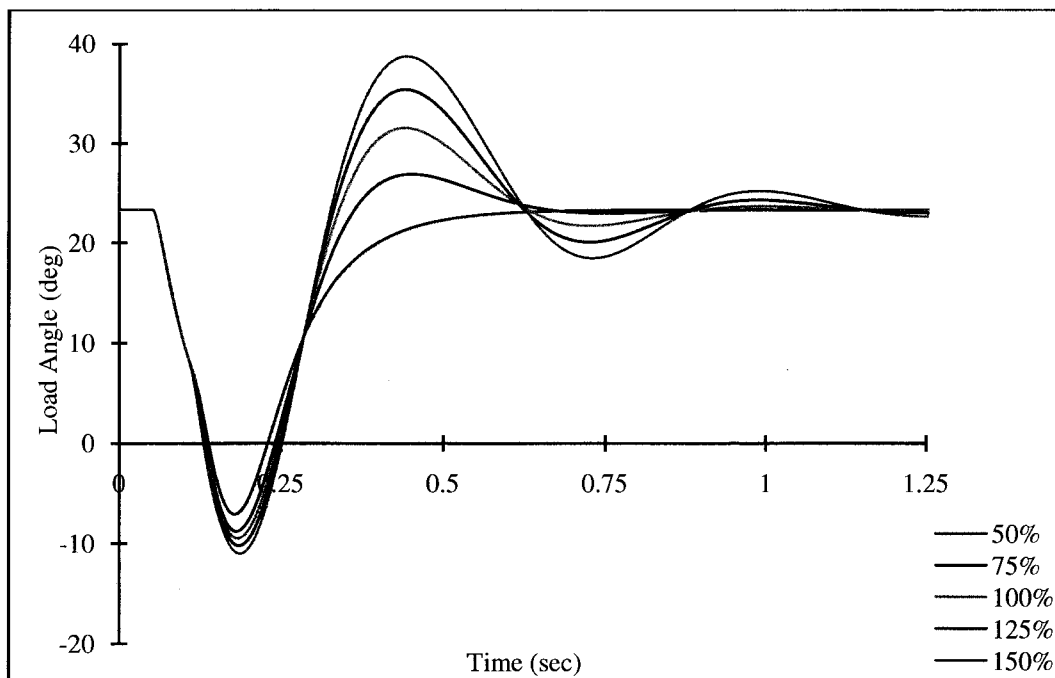


Fig. 4.15. Swing in the load angle for different q-axis damper circuit resistance.

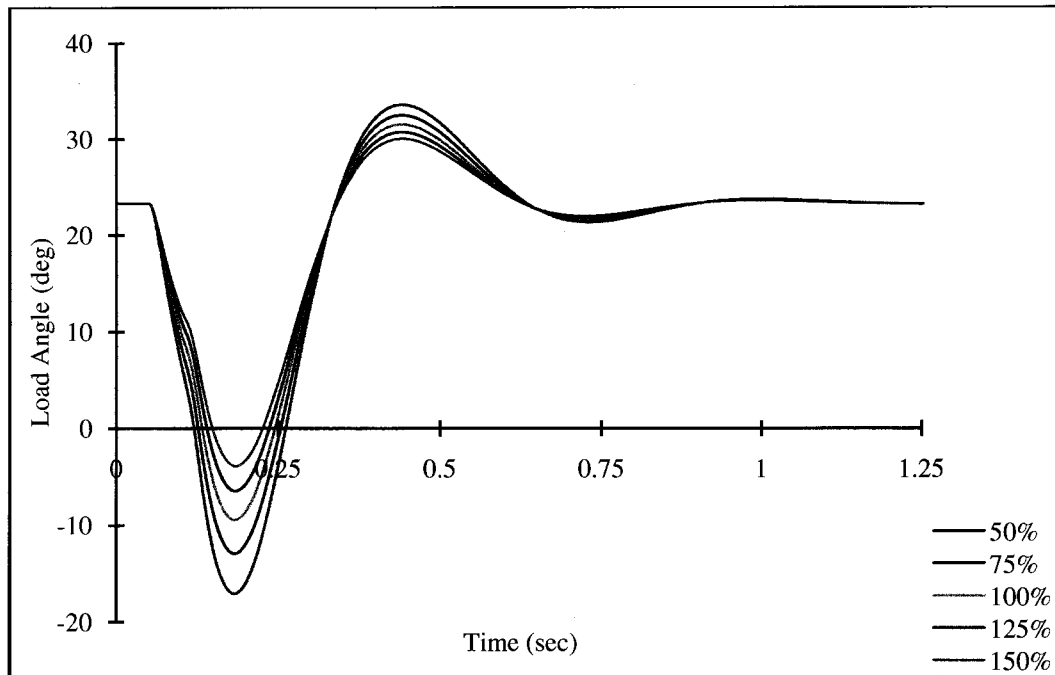


Fig. 4.16. Swing in the load angle for different d-axis damper circuit reactance.

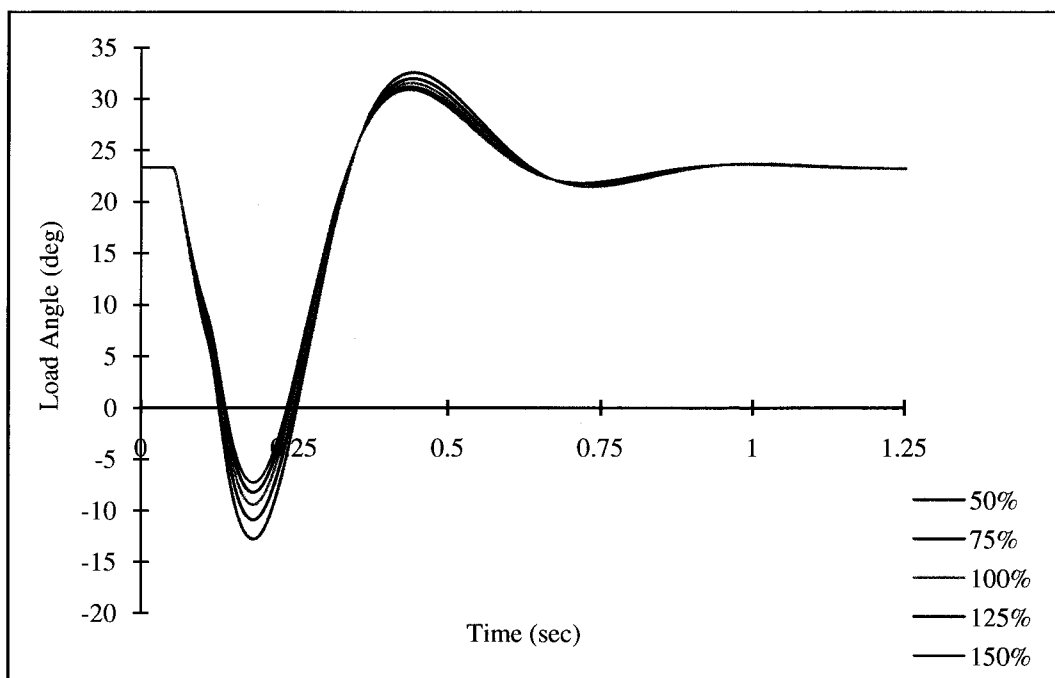


Fig. 4.17. Swing in the load angle for different q-axis damper circuit reactance.

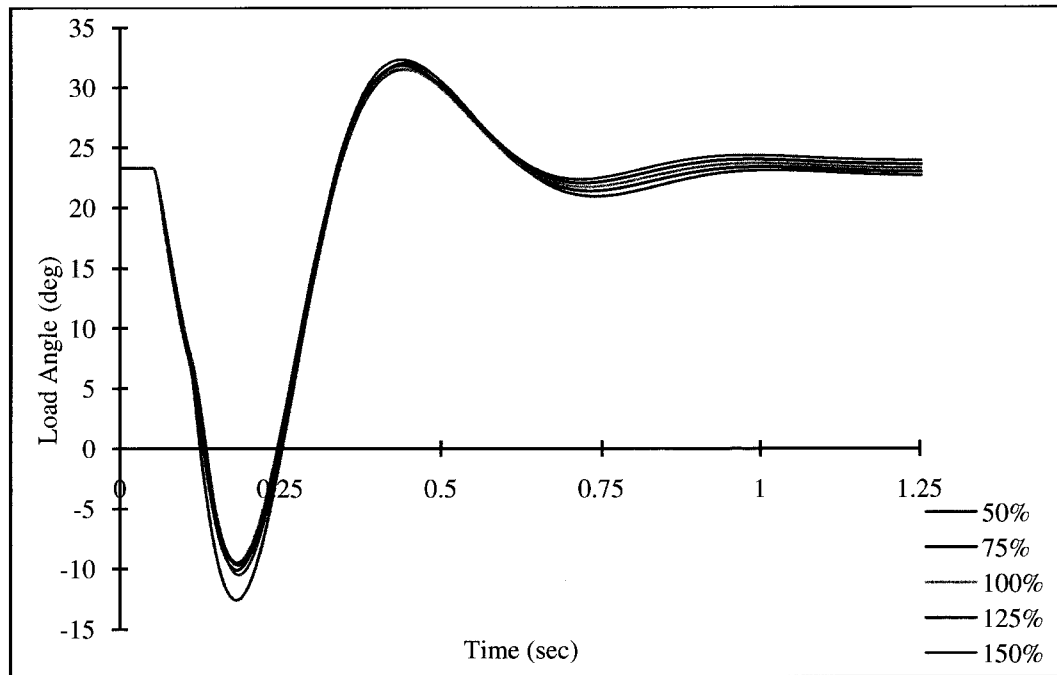


Fig. 4.18. Swing in the load angle for different armature winding resistance.

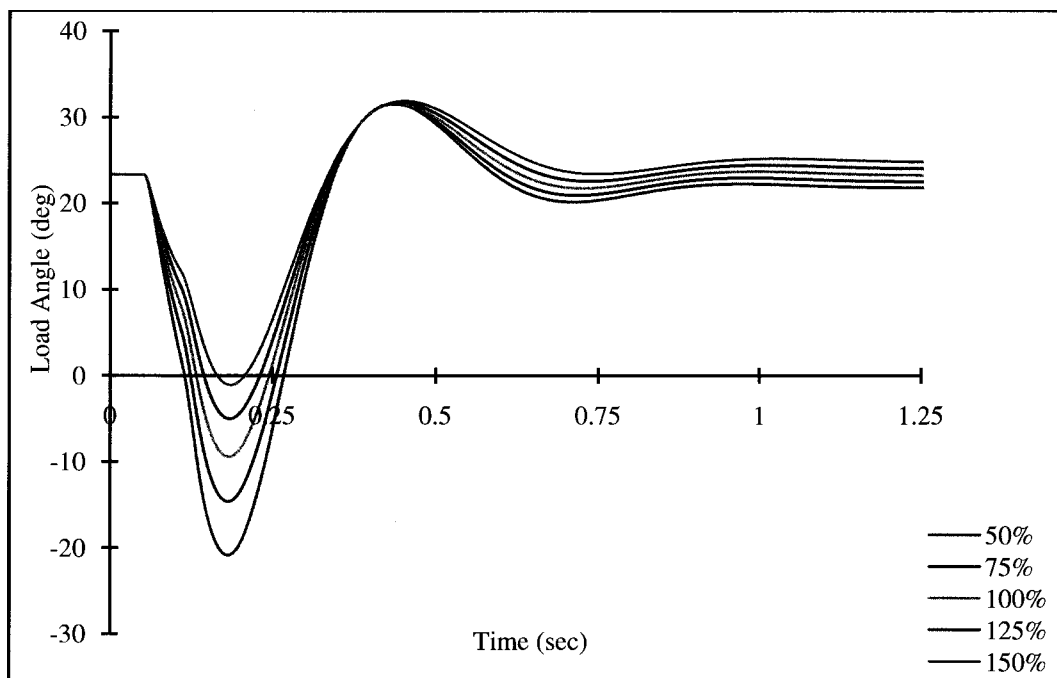


Fig. 4.19. Swing in the load angle for different leakage reactance.

From the load angle sensitivity analysis to transient model of self-excited synchronous reluctance generator, it has been found that load angle is most sensitive to d-axis damper circuit resistance as compared to other parameters of the machine. The machine parameters as shown in Table: 4.3 are ranked according to load angle sensitivity.

Table 4.3
Summary of results: Load angle sensitivity

Machine Parameters (pu)	Ave. Load Angle (deg)
d-axis damper circuit resistance (R_{kd1})	42°
Armature resistance (R_a)	41.33°
Leakage reactance (X_l)	39°
d-axis damper circuit reactance (X_{kd1})	38.5°
q-axis damper circuit reactance (X_{kq1})	38.33°
q-axis damper circuit resistance (R_{kq1})	38°

5 CONCLUSIONS

This research work presents a comprehensive study of a self-excited synchronous reluctance generator that includes the steady-state and transient analyses of the machine. The machine has been modeled for stability analysis using voltages, currents, mechanical, electromagnetic torque and capacitor current equations. A capacitor bank was used for self-excitation. The effect of saturation has been considered in order to predict more accurate results.

A new linearized mathematical model of a self-excited synchronous reluctance generator for stand-alone operation has been developed. The state-matrix of the system has been used to obtain the eigenvalues for steady-state stability analysis. The effects of different loading conditions on the system steady-state stability have been explained. It has been found that the system moves towards instability with the increase in output power.

Transient stability analysis has also been performed on the machine. The transient variations of load angle, rotor speed, electromagnetic torque, stator currents, rotor currents, and stator and rotor fluxes have been analyzed. The machine has been tested for different fault durations in the stable operating region, marginally stable and unstable regions of the system have been explained. It has been found that the system becomes unstable at longer duration of faults.

Moreover, a sensitivity analysis has been performed in order to understand the effect of the machine equivalent circuit parameters on the steady-state and transient stability analyses. Machine parameters were varied from 50% to 150% of their standard values.

The results can be summarized as follows:

- The steady-state model is applied to a three-phase 0.37 kW synchronous reluctance machine for stability analysis.
- With the increase in active, reactive and apparent power output, the system moves towards instability.
- The excitation capacitance has a profound effect on the machine performance.
- The eigenvalue sensitivity has been analyzed on the steady-state model and of the machine parameters ranked accordingly.

- The transient stability has been analyzed by employing a symmetrical three-phase short-circuit fault across the machine terminals.
- The load angle sensitivity has been analyzed and the machine parameters have been ranked according to their load angle sensitivity.
- For more reliable performance of a self-excited synchronous reluctance generator, it is recommended to consider quadrature axis saturation and cross-magnetization effect in the machine modeling for both the steady-state and transient stability analyses.

LIST OF PUBLICATIONS

- [1] S. Rana and N. C. Kar, "Steady-state analysis of self-excited synchronous reluctance generator," presented at the *2008 IEEE Canadian Conference on Electrical & Computer Engineering*, Niagara Falls, and May.

VITA AUCTORIS

NAME: Salah-ud-Din Rana
PLACE OF BIRTH: Kasur, Pakistan
YEAR OF BIRTH: 1963
EDUCATION: University of Engineering & Technology
Lahore, Pakistan
1984-1989 B.Sc. in Electrical Engineering

University of Engineering & Technology
Lahore, Pakistan
1996-1998 M.Sc. in Electrical Engineering

University of Windsor
Windsor, Ontario
2007-2009, MSc. in Electrical Engineering